evidenced by Katori and Hofbauer, and further in view of Barnes, et al., U.S. Patent No. 5,506,211.

The Examiner has imposed a new rejection of claims 2-8, 10-11, and 13-22 under 35 U.S.C. § 103(a) as being unpatentable over Bok, et al., WO 98/16220 ("Bok WO") in view of Kim, WO 02/17909 ("Kim") and further in view of Bok, U.S. Patent Application Publication 2001/0014669 ("Bok US"). The Examiner has argued that Bok WO teaches pharmaceutical compositions comprising hesperidin for inhibiting HMG-CoA reductase activity in mammals. The Examiner acknowledges that Bok WO does not teach the use of hesperidin in a method for stimulating bone formation and/or inhibiting bone resorption and treating associated diseases (Office Action, p. 4).

In order to overcome this deficiency, the Examiner relies on Kim, which teaches a therapeutic agent for osteoporosis comprising quercetin derivatives. Kim's therapeutic agent stimulates osteoblast proliferation and inhibits osteoclast proliferation. The Examiner has also stated that Bok US teaches a method of inhibiting the activity of HMG CoA reductase in mammals with the administration of quercetin. Thus, the Examiner concludes as follows:

> "It would have been obvious to one of ordinary skill in the art...to have employed hesperidin, which is an HMG CoA reductase inhibitor as taught by [Bok WO], as a treatment agent for bone disorders, namely osteoporosis. One would be motivated to employ hesperidin for such therapeutic applications because Kim teaches that quercetin, a bioflavanoid differing from hesperidin by a hydroxyl moiety, is employed as a therapeutic agent for osteoporosis. The nexus between the two compounds is brought together by Bok (US) which teaches that quercetin is also an HMG CoA reductase inhibitor. Additionally, as is well known in the art and document by Bok (US), quercetin and hesperidin are readily found in citrus fruit. Thus, because both hesperidin and quercetin are bioflavanoids and found from the same natural sources and further are found to be HMG CoA reductase inhibitors, then one would expect, with a reasonable degree of success that if

> quercetin is an possessing the therapeutic potential of treating osteoporosis, then it would be likely that hesperidin would also be likely to have such potential and would be equally successful in treating such bone disorders, in the absence of unexpected results."

(Office Action, pp. 5-6). Thus, in essence, the Examiner's position is that (1) Bok WO teaches that hesperidin is an HMG CoA reductase inhibitor; (2) Kim teaches that a composition comprising quercetin can be used to treat osteoporosis; (3) Bok US teaches that quercetin is also an HMG CoA reductase inhibitor, and (4) since quercetin and hesperidin are bioflavonoids which only differ by an hydroxyl moiety and which are both inhibitors of HMG-CoA, one skilled in the art would expect that the hesperidin is an anti-osteoporosis agent. Applicants respectfully traverse.

First, none of the cited art teaches or alludes that HMG-CoA reductase is involved in bone resorption and/or in bone formation. In fact, Bok WO teaches that HMG-CoA reductase is involved in hyperlipidemia, artheriosclerosis, angina pectoris, stroke and hepatic diseases. Such diseases are clearly different from osteoporosis. Nothing in Bok WO, or either of the other references, would lead one of skill in the art to reasonably expect that a compound which inhibits HMG-CoA reductase could have an effect on bone resorption and/or bone formation.

Second, contrary to the Examiner's contention, quercetin and hesperidin are structurally very distinct. Quercetin is an aglycone flavonol whereas hesperidin is a glycone flavanone. As shown below, hesperidin differs from quercetin by (i) the presence of a glycosyl group, by (ii) the presence of a methyl group on one of its phenol functions and (iii) by the absence of an enol group (which corresponds to a hydroxyl group conjugated with a double bond):

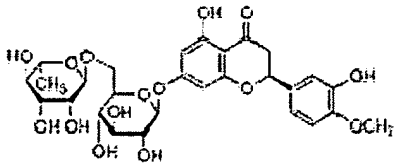

Hesperidin

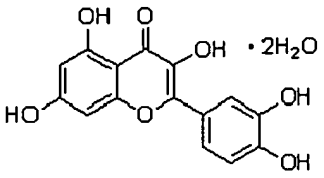

Quercetin

Since hesperidin and quercetin are so structurally distinct, one skilled in the art would not reasonably expect that these two molecules would have similar biological profiles, particularly with respect to bone resorption and/or bone formation.

Third, quercetin and hesperidin do in fact have distinct and different biological profiles. As expected in view of their different chemical structures, numerous publications show that quercetin and hesperidin have different biological activities. For example, the following publications, copies of which are attached for the Examiner's convenience, show different biological properties for the two compounds:

a) Choi *et al.* (*The Journal of Nutrition*, 2003, **133**: 985-991) ("Choi") teaches that flavonoids differ in their antiapoptotic efficacy in hydrogen peroxide-treated vascular endothelial cell model. The flavanones (hesperidin and naringin) do not have cytoprotective effects whereas (-) epigallocatechin gallate and quercetin inhibit endothelial apoptosis, enhanced the expression of bcl-2 protein and inhibited the expression of bax protein, the cleavage and the activation of caspase-3 (see Abstract). In a cell-free system, hesperidin is totally inefficient to scavenge DPPH radical (SC50>100 μmol/l) whereas quercetin exhibits a SC50 of 5.0 μmol/l (see Table 1, p. 987). Choi concludes that this endothelial cell model demonstrates that there are differences in antiapoptotic capacity among flavonoids, which appears to stem from their disparate chemical structures (see left column p.990)

b) Li *et al* (*Drug Metabolism and Disposition,* 2007, 35:1203-1208) ("Li") relates to the ability of different flavonoids to inhibit esterase. Li teaches that glycoside flavonoids such as hesperidin do not inhibit the hydrolysis of PNPA (p-nitrophenylacetate) by purified porcine esterase and human liver microsomes whereas the flavonoid aglycones such as quercetin, show appreciable inhibition of PNPA hydrolysis in purified porcine esterase, and human and rat liver systems (see Abstract and Table 1).

c) Rotelli *et al* (*Pharmacological Research*, 2003, 48, 601-606) ("Rotelli") relates to the anti-inflammatory activities of flavonols (quercetin, rutin and morin) and flavanones (hesperetin and hesperidin) on different animal models of acute and chronic inflammation. In the carrageenan-induced paw model, hesperidin has no activity whereas quercetin significantly reduces the paw oedema (see Table 1 p. 603). In the xylene-induced ear swelling model, hesperidin exerts a significant anti-inflammatory effect whereas quercetin slightly inhibits the oedema (see Table 2, p.604). Finally, in the pellet granuloma model, both quercetin and hesperidin significantly reduce granuloma formation (see Table 3 p.604).

In view of the results reported in these papers, it is apparent that the anti-inflammatory activities of flavonoïd compounds such as quercetin and hesperidin are different, unpredictable and uncorrelated.

Because of the distinct structures and properties of the two compounds, a person of skill in the art would consider that the inhibition of HMG-CoA reductase by both quercetin and hesperidin is just a coincidence. One skilled in the art would not expect with a reasonable degree of success that hesperidin may act as an anti-osteoporosis agent even if quercetin does.

Finally, it should be emphasized that the activity of quercetin and that of hesperidin derivatives on bone metabolism are very different. Applicants have shown that hesperidin derivatives do not affect the proliferation of osteoblasts (see Trzeciakiewicz *et al.*, *J. Agric. Food Chem.* 2010, 58, 668-675, (copy attached), Abstract) whereas Kim teaches that quercetin stimulates osteoblast proliferation.

Accordingly, a person of skill in art would not have had any reason to believe, based on the disclosures of Bok WO, Kim, and Bok US, that hesperidin would be used in a method for stimulating bone formation and/or inhibiting bone resorption. Therefore, applicants respectfully request that the § 103 rejection be reconsidered and withdrawn.

Conclusion

In view of the foregoing, this application is now in condition for allowance. If the examiner believes that an interview might expedite prosecution, the examiner is invited to contact the undersigned.

Respectfully submitted,

JACOBSON HOLMAN PLLC

By: _____
Allen S. Melser
Reg. No. 27,215

400 Seventh Street, N. W.
Washington, D.C. 20004
Telephone: (202) 638-6666
Date: February 25, 2009

Polyphenolic Flavonoids Differ in Their Antiapoptotic Efficacy in Hydrogen Peroxide–Treated Human Vascular Endothelial Cells[1]

Yean-Jung Choi, Jung-Sook Kang,* Jung Han Yoon Park, Yong-Jin Lee, Jung-Suk Choi and Young-Hee Kang[2]

*Division of Life Sciences and Silver Biotechnology Research Center, Hallym University, Chuncheon, Korea and *Food and Nutrition, Cheju University, Cheju, Korea*

ABSTRACT Oxidative injury induces cellular and nuclear damage that leads to apoptotic cell death. Agents or antioxidants that can inhibit production of reactive oxygen species can prevent apoptosis. We tested the hypothesis that flavonoids can inhibit H_2O_2-induced apoptosis in human umbilical vein endothelial cells. A 30-min pulse treatment with 0.25 mmol/L H_2O_2 decreased endothelial cell viability within 24 h by ~40% ($P < 0.05$) with distinct nuclear condensation and DNA fragmentation. In the H_2O_2 apoptosis model, the addition of 50 μmol/L of the flavanol (-)epigallocatechin gallate and the flavonol quercetin, which have in vitro radical scavenging activity, partially ($P < 0.05$) restored cell viability with a reduction in H_2O_2-induced apoptotic DNA damage. In contrast, the flavones, luteolin and apigenin, at the nontoxic dose of 50 μmol/L, intensified cell loss ($P < 0.05$) after exposure to H_2O_2 and did not protect cells from oxidant-induced apoptosis. The flavanones, hesperidin and naringin, did not have cytoprotective effects. The antioxidants, (-)epigallocatechin gallate and quercetin, inhibited endothelial apoptosis, enhanced the expression of bcl-2 protein and inhibited the expression of bax protein and the cleavage and activation of caspase-3. Therefore, flavanols and flavonols, in particular (-)epigallocatechin gallate and quercetin, qualify as potent antioxidants and are effective in preventing endothelial apoptosis caused by oxidants, suggesting that flavonoids have differential antiapoptotic efficacies. The antiapoptotic activity of flavonoids appears to be mediated at the mitochondrial bcl-2 and bax gene level. J. Nutr. 133: 985–991, 2003.

KEY WORDS: • *flavonoids* • *endothelial apoptosis* • *hydrogen peroxide* • *bcl-2* • *caspase-3*

Apoptosis, a morphologically and biochemically distinct form of cell death characterized by cell shrinkage without membrane ruptures, cell membrane blebbing, nuclear chromatin condensation and nonrandom DNA fragmentation, is indispensable for physiologic development and homeostasis of tissues and the elimination of diseased cells in multiorganisms (1,2). Defects in apoptosis have been implicated in neurodegenerative diseases, cancer and autoimmune diseases (2,3). Oxidative injury after diverse stimuli including clinical and experimental ischemia/hypoxia, reperfusion and inflammation can induce cardiac and endothelial cell apoptosis (4–7), which is a fundamentally different mode of cell death from necrosis. The severity of cellular damage by an oxidant injury determines which mechanism of cell death dominates (8). Accordingly, agents or antioxidants that can inhibit production of reactive oxygen species (ROS)[3] can prevent apoptosis (4,9,10). However, the underlying molecular mechanisms by which antioxidative agents protect cells from stimulator-triggered apoptosis remain to be elucidated.

There is currently intense interest in polyphenolic phytochemicals such as flavonoids, proanthocyanidins and phenolic acids. Epidemiologic studies have shown that a high consumption of these polyphenolics is inversely related to the risk of cardiovascular diseases (11–13), and this phenomenon appears to be associated with their antioxidant capacity (14). Flavonoids constitute one of the antioxidant phytochemical groups and are found in a large number of fruits and vegetables. There are several subclasses such as flavonols, flavones, isoflavones, flavonones, flavan-3-ols and anthocyanidins. These flavonoids are natural antioxidants that scavenge various types of radicals in aqueous and organic environments (15–21), and anti-inflammatory agents that inhibit adhesion molecules and matrix proteases (22–24). Whether these flavonoids act in vivo as antioxidants or anti-inflammatory agents appears to depend on their bioavailabilities.

On the basis of the literature evidence that flavonoids are antioxidants and have the ability to scavenge free radicals, we examined the effects of these polyphenolic compounds, when applied in submillimolar doses, on apoptosis in H_2O_2-exposed

[1] Supported by Grant R05-2000-000-00205-0 from Korea Science and Engineering Foundation and Grant R12-2001-007202-0 from Korea Science and Engineering through the Silver Biotechnology Research Center at Hallym University, and in part by the Hallym Academy of Sciences at Hallym University, Korea (2002-19-1).

[2] To whom correspondence should be addressed.
E-mail: yhkang@hallym.ac.kr.

[3] Abbreviations used: DMSO, dimethyl sulfoxide; DPPH, 1,1-dipheny-2-picrylhydrazyl; FBS, fetal bovine serum; HUVEC, human umbilical vein endothelial cells; Ig, immunoglobulin; MTT, 3-(4,5-dimetylthiazol-yl)-diphenyl tetrazolium bromide; NBT, nitro blue tetrazolium; ROS, reactive oxygen species; SC_{50}, half-maximal scavenging concentration; TBS-T, Tris buffered saline-Tween 20; TUNEL, terminal deoxynucleotidyl transferase-mediated dUTP nick end labeling.

0022-3166/03 $3.00
Manuscript received 16 September 2002. Initial review completed 23 October 2002. Revision accepted 10 December 2002.

human umbilical vein endothelial cells (HUVEC). Cells were exposed to H_2O_2 for 30 min, killing 40% of cells within 24 h. It has been shown that there are differences in the antioxidant capacity among different groups of flavonoids and within each group of flavonoids (16,25). By measuring cell viability, nuclear morphology, DNA fragmentation and apoptotic gene protein expression, we assessed the antiapoptotic efficacy of various polyphenolic compounds in the vascular endothelium model. To elucidate the capacity of polyphenolic compounds to inhibit oxidant-induced apoptosis, four different subclasses of polyphenolic flavonoids were used, i.e., flavanols [(-)epigallocatechin gallate and (+)catechin]; flavonols (quercetin and myricetin); flavanones (naringin and hesperidin); and flavones (luteolin and apigenin).

MATERIALS AND METHODS

Chemicals. Fetal bovine serum (FBS), penicillin-streptomycin, and all cell growth supplements were purchased from Clonetics (San Diego, CA). Polyphenolic flavonoids [flavanols, (-)epigallocatechin gallate and (+)catechin; flavonols, quercetin and myricetin; flavanones, naringin and hesperidin; and flavones, luteolin and apigenin], M199 chemicals, and 3-(4,5-dimetylthiazol-yl)-diphenyl tetrazolium bromide (MTT) were obtained from Sigma Chemical (St. Louis, MO) as were all other reagents, unless specifically stated elsewhere. All flavonoids were solubilized by dimethyl sulfoxide (DMSO) for culturing with cells (26); the final culture concentration of DMSO was ≤5 g/L.

Measurement of DPPH radical scavenging activity. The radical scavenging activity of flavonoids was assayed using a stable free radical, 1,1-dipheny-2-picrylhydrazyl (DPPH) by a previously reported method (27) with minor modifications. A methanol solution (100 μL) of each flavonoid at different concentrations (10–350 μmol/L) was added to the mixture of 100 mmol/L Tris-HCl buffer (pH 7.4) and 0.2 mmol/L DPPH in methanol. The solution was mixed vigorously and kept for 20 min in the dark. The free radical scavenging activity of each flavonoid was quantified by the decolorization of DPPH at 517 nm. The antioxidant power of flavonoids was expressed as half-maximal scavenging concentration (SC_{50}, their concentration decreasing DPPH 50%).

Primary culture of human vascular endothelial cells. HUVEC were isolated using collagenase (Worthington Biochemical, Lakewood, NJ), as described elsewhere (28). Cultures were maintained at 37°C in a humidified atmosphere of 5% CO_2 in air. Cells were incubated in 25 mmol/L HEPES-buffered M199 containing 10% FBS, 2 mmol/L glutamine, 100,000 U/L penicillin, 100 mg/L streptomycin and growth supplements (0.9 g/L bovine brain extract, 0.75 g/L human epidermal growth factor and 75 mg/L hydrocortisone). Cells were passaged at confluence and used within 4–5 passages. Cells were subcultured at 70–80% confluence. Endothelial cells were identified by their cobblestone morphology and uptake of fluorescently labeled acetylated LDL [1.1′-dioctadecyl-3,3,3′,3′-tetramethylindocarbocyanine perchlorate; Molecular Probes, Eugene, OR; (28)].

To determine the dose-viability response of the tested flavonoids, HUVEC were cultured in 25 mmol/L HEPES-buffered M199 containing 10% FBS and 10–100 μmol/L of each tested flavonoid for 24 h.

H_2O_2-induced oxidant stress. The cells were preincubated for 30 min with 50 μmol/L of each tested flavonoid, and then incubated for another 30 min with media containing an additional 0.25 mmol/L H_2O_2. In H_2O_2 incubations, H_2O_2 was detoxified by adding catalase (100,000 U/L, Worthington Biochemical) at the end of the 30-min incubation period; this terminated all activity of extracellular H_2O_2. Non-H_2O_2–treated control cells were incubated in the same way as those used in the H_2O_2 protocols. Cells were washed thoroughly with PBS and then resupplied with fresh H_2O_2-free medium containing 50 μmol/L of the tested flavonoid. Incubation was continued for another 24 h before biochemical and molecular analyses were performed.

Cell viability. At the end of the 24 h incubation period, the MTT assay was performed to quantitate cellular viability (30). HUVEC were incubated in fresh medium containing 1 g/L MTT for 3 h at 37°C. After removal of unconverted MTT, the purple formazan product was measured colorimetrically at λ = 570 nm with background subtraction at λ = 690 nm.

Nuclear morphology. Nuclear morphology was examined by fluorescence microscopy with an Olympus BX50 fluorescent microscope (Olympus Optical Co., Tokyo, Japan) equipped for fluorescence illumination and for photomicroscopy. After the fixation of HUVEC with ice-cold 4% formaldehyde for 1 h, the nuclear stain Hoechst 33258 (Molecular Probes) was added at a final concentration of 10 mg/L for 15 min to allow uptake and equilibration before microscopic observation. The coverslips were mounted while wet in aqueous mounting solution. Cells containing fragmented or condensed nuclei were considered apoptotic, whereas those containing diffuse and irregular nuclei were considered necrotic (31).

In situ cell death detection (TdT-mediated dUTP nick end labeling, TUNEL). DNA strand breaks were detected using the nick-end labeling technique (32). To detect in situ DNA fragmentation, the TUNEL assay with HUVEC was performed following a previously published method (34). Cultured cells were labeled using a commercially available end-labeling kit (Boehringer Mannheim, Mannheim, Germany). For the detection and visualization, extra-avidin–conjugated alkaline phosphatase was introduced in an alkaline phosphatase substrate buffer (100 mmol/L Tris-HCl, 5 mmol/L $MgCl_2$, pH 9.5) containing nitro blue tetrazolium (NBT; 50 g/L in 70% dimethylformamide) and bromochloroindolyl phosphate toluidine (50 g/L in 70% dimethylformamide). Photomicroscopy took place under a cover slide with a Olympus CH2 light microscope.

Agarose gel electrophoresis. The calcium-activated endonuclease produces well-defined DNA fragments (33), which can be detected as a DNA ladder on agarose gels. Extraction and electrophoresis of genomic DNA were performed according to methods published elsewhere (34). DNA from HUVEC was isolated using 5 g/L sodium N-lauroyl sarcosinate, 10 g/L proteinase K and 10 mg/L RNase A. DNA samples were electrophoresed on a 1.8% agarose gel containing ethidium bromide (0.5 mg/L). For apoptotic alterations to DNA integrity, DNA bands were visualized using an UV transilluminator (Hoefer Scientific Instrument, San Francisco, CA), and photographs of gels were obtained using Polaroid Type 667 positive/negative film (Polaroid Co., Wayland, MA).

Immunocytochemistry. After endothelial cells were thoroughly washed with Tris buffered saline (TBS), cells were incubated for 20 min with 10% normal goat serum in TBS to block any nonspecific binding. After fixed cells were washed twice with TBS, monoclonal mouse bcl-2 antibody (1:100 dilution in TBS; BD Transductional, San Diego, CA) was added to cells and incubated overnight at 4°C. Cells were washed with TBS and incubated with a fluorescein isothiocyanate–conjugated goat anti-mouse immunoglobulin (Ig)G (1:200 dilution in TBS; Sigma) as a secondary antibody. Images were obtained by a fluorescence microscopy with an Olympus BX51 fluorescent microscope.

Western blot analysis. Whole-cell extracts were prepared from HUVEC in a lysis buffer containing 10 g/L β-mercaptoenthanol, 1 mol/L β-glycerophosphate, 0.1 mol/L Na_3VO_4, 0.5 mol/L NaF and protease inhibitor cocktail. Cell lysates containing equal amounts of total protein were fractionated by electrophoresis on 12 or 15% SDS-PAGE gels and transferred onto a nitrocellulose membrane. Nonspecific binding was blocked by soaking the membrane in a TBS-T buffer [0.5 mol/L Tris-HCl (pH 7.5), 1.5 mol/L NaCl, and 1 g/L Tween 20] containing 50 g/L nonfat dry milk for 3 h. The membrane was incubated for 3 h with a primary antibody [monoclonal mouse anti-human bcl-2 (1:500 dilution; Santa Cruz Biotechnology, Santa Cruz, CA), monoclonal mouse anti-human bax (1:500 dilution; BD Transductional), or polyclonal rabbit anti-human caspase-3 (1:1000 dilution; Cell Signaling Technology, Beverly, MA)]. After five washes with TBS-T, the membrane was then incubated for 1 h with a goat anti-mouse IgG or a goat anti-rabbit IgG conjugated to horseradish peroxidase (1:10,000 dilution, Jackson ImmunoResearch, West Grove, PA). The levels of bcl-2 and bax proteins and caspase-3 protein were determined using Supersignal West Pico chemiluminescence detection reagents (Pierce, Rockford, IL) and Konica X-ray film (Konica, Tokyo, Japan). Incubation with

polyclonal rabbit β-actin antibody (1:1000 dilution, Santa Cruz Biotechnology) was also performed for the comparative control.

Statistical analysis. The results are presented as mean ± SEM. Statistical analyses were conducted using SAS statistical software package version 6.12 (SAS Institute, Cary, NC). One-way ANOVA was used to determine effects of both H_2O_2 and individual flavonoids. The differences among treatment groups were analyzed with Duncan's multiple range test and were considered significant at $P < 0.05$.

RESULTS

DPPH radical scavenging activity. Among the tested flavonoids in the cell-free system, the flavanols, (-)epigallocatechin gallate and (+)catechin, and the flavonols, quercetin and myricetin, had high DPPH scavenging activities with half-maximal scavenging concentrations, SC_{50}, lower than 10 μmol/L (Table 1). These compounds were more potent than L-ascorbic acid, the classic reference antioxidant, with 14.0 μmol/L SC_{50}. In contrast, the flavanones, naringin and hesperidin, and the flavones, luteolin and apigenin, were not active even at concentrations up to 100 μmol/L.

Endothelial cell viability under the influence of H_2O_2. Except for apigenin, all other flavonoids tested showed little cytotoxicity even at 100 μmol/L when incubated with cells for 24 h, but at concentrations ≤50 μmol/L, apigenin did not significantly decrease cell viability ($P > 0.05$, data not shown). Accordingly, the maximal nontoxic concentration of all the flavonoids used for culture experiments was 50 μmol/L. During 24-h incubations, the cytotoxicity of H_2O_2 increased dose dependently at concentrations ranging from 0.05 to 0.25 mmol/L with a decrease in cell viability by 40% at 0.25 mmol/L. Data in tables and figures were obtained when HUVEC were treated with 0.25 mmol/L H_2O_2 for 30 min (Fig. 1, *upper panel*).

Each flavonoid inhibited H_2O_2-induced cell death differently (Fig. 1, *lower panel*). Among all of the flavonoids tested, 50 μmol/L (-)epigallocatechin gallate and quercetin reduced the rate of H_2O_2-induced cell death, whereas equimillimolar luteolin and apigenin significantly aggravated the H_2O_2-induced cytotoxicity ($P < 0.05$). On the other hand, the cell viability reduced by 0.25 mmol/L H_2O_2 was not affected by (+)catechin, myricetin and the flavanones, naringin and hesperidin (Fig. 1, *lower panel*).

Nuclear condensation and DNA fragmentation. The H_2O_2 produced cells that exhibited fragmented and/or condensed nuclei within 24 h and there were nonnucleated cell

TABLE 1

Radical scavenging activity of flavonoids in a cell-free system[1]

Flavonoids	SC_{50}[2]
	μmol/L
(−)epigallocatechin gallate	3.0 ± 0.2
quercetin	5.0 ± 0.1
(+)catechin	6.4 ± 0.4
myricetin	6.6 ± 0.3
hesperidin	>100
naringin	>100
luteolin	>100
apigenin	>100
L-ascorbic acid	14.0 ± 0.6

[1] Values are mean ± SEM, n = 5–8.
[2] SC_{50} represents flavonoid concentrations decreasing 0.2 mmol/L DPPH in methanol (1:2, v/v) to 50%.

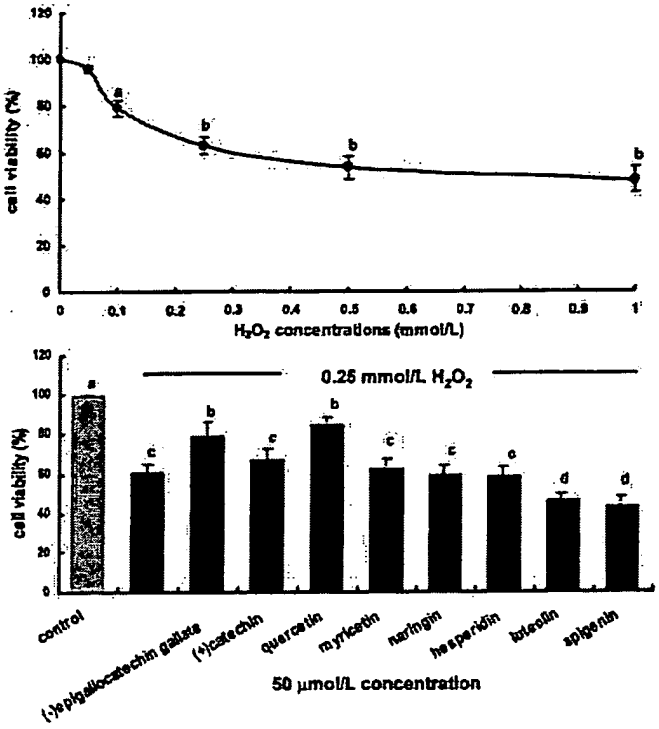

FIGURE 1 Human umbilical vein endothelial cell (HUVEC) viability after H_2O_2-induced oxidant stress. The *upper panel* shows the 24-h viability of cells treated with ≤1.0 mmol/L H_2O_2 for 30 min. Values are mean ± SEM, n = 4 and are expressed as the percentage of cell survival relative to the H_2O_2-free control cells (viability = 100%). The *lower panel* shows the viability of cells treated with a 0.25 mmol/L H_2O_2 pulse and incubated with 50 μmol/L of various flavonoids. Values are mean ± SEM, n = 4 and are expressed as the percentage of cell survival relative to H_2O_2-untreated control cells (viability = 100%). Means not sharing a letter differ, $P < 0.05$.

fragment apoptotic bodies (Fig. 2, arrows in microphotographs with Hoechst 33258 nuclear stain). In the H_2O_2-untreated control cells, no signs of morphological nuclear damage or chromatin condensation were observed (Fig. 2). The nuclear morphology of cells exposed to H_2O_2 with (-)epigallocatechin gallate, (+)catechin or quercetin was comparable to, if not indistinguishable from that of the H_2O_2-untreated control cells. In marked contrast, the morphology of cells treated with H_2O_2 in the presence of luteolin or apigenin compared poorly with that of the H_2O_2-untreated cells but well with that of cells treated with H_2O_2 alone. In cells exposed to H_2O_2 and incubated with luteolin and apigenin, cell density was markedly reduced and nuclear condensations and appearance of apoptotic body–like structures became increasingly frequent in response to H_2O_2 (Fig. 2).

When the in situ TUNEL technique for assessing oxidant DNA damage was applied, there was the expected lack of staining in the H_2O_2-untreated control cells (Fig. 3). However, heavy nuclear staining in cells exposed to H_2O_2 alone was observed. H_2O_2-exposed cells treated with (-)epigallocatechin gallate, (+)catechin or quercetin had substantial, but not complete disappearance of nuclear DNA fragmentation. The other flavonoids did not reduce but rather intensified the TUNEL staining, especially luteolin and apigenin.

The results of nuclear condensation (Fig. 2) and of DNA fragmentation (Fig. 3) assays suggested that (-)epigallocatechin gallate and quercetin but not luteolin and apigenin

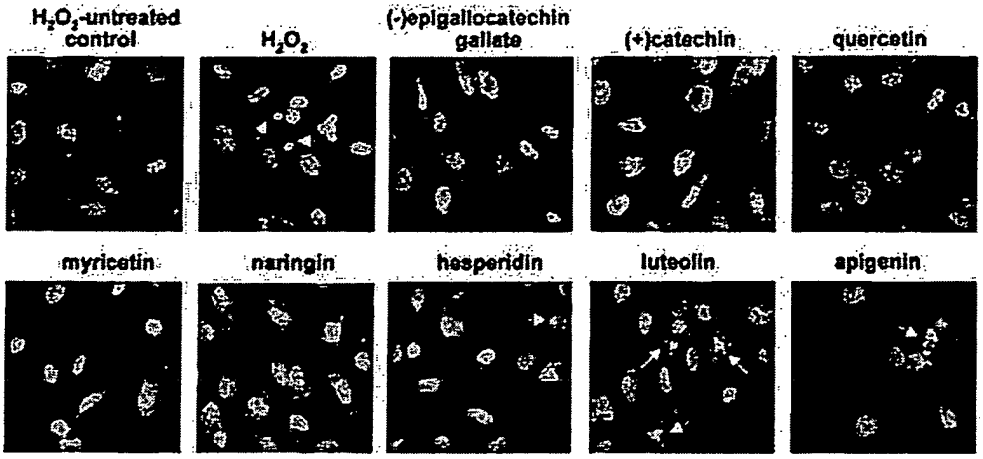

FIGURE 2 Typical effects of 0.25 mmol/L H_2O_2 in the absence and presence of 50 μmol/L flavonoids on nuclear morphology of human umbilical vein endothelial cells (HUVEC) stained with Hoechst 33258. H_2O_2 caused nuclear condensation and the appearance of apoptosis-like bodies (arrows). This is representative of 5 independent slides. Magnification: X400.

inhibited H_2O_2-induced apoptosis in the vascular endothelium. DNA laddering tests for oxidant DNA damage supported this notion. DNA isolated from HUVEC treated with H_2O_2 alone exhibited a distinct DNA ladder pattern (Fig. 4). DNA fragments were substantially but not fully alleviated when H_2O_2-treated cells were treated with 50 μmol/L (-)epigallocatechin gallate, (+)catechin and quercetin. In contrast, no protection against internucleosomal DNA fragmentation was observed in the luteolin- and apigenin-treated cells (Fig. 4), indicating further induction of apoptosis.

Expression of bcl-2 and bax proteins and activation of caspase-3. Immunostaining assays were used to compare the effects of the selected flavonoids on expression of bcl-2 in the presence of H_2O_2. As expected, there was substantial cytoplasmic staining in the H_2O_2-free control cells, whereas this staining did not occur in cells exposed to H_2O_2 alone, suggesting the down-regulation of bcl-2 expression at the single cell level (Fig. 5). However, addition of (-)epigallocatechin gallate or quercetin to H_2O_2-exposed cells increased the staining of bcl-2. In marked contrast, the flavone apigenin did not increase the expression of bcl-2 reduced by H_2O_2, suggesting that not all of the flavonoids can attenuate H_2O_2-induced apoptotic gene expression in the vascular endothelium.

Similar Western blot results for the bcl-2 protein expression of HUVEC were obtained (Fig. 6). There was relatively weak or undetectable expression of bax protein in H_2O_2-untreated control cells. The bax protein was obviously up-regulated in H_2O_2-injured cells relative to the untreated quiescent cells. When H_2O_2-injured cells were treated with (-)epigallocatechin gallate or quercetin, the expression of endothelial bax protein markedly decreased (Fig. 6). Treatment with apigenin did not inhibit bax protein expression.

Western blot analysis showed that a 30-min pulse treatment with H_2O_2 caused caspase-3 cleavage in HUVEC within 24 h, but this effect was partially blocked by (-)epigallocatechin gallate and fully blocked by quercetin (Fig. 6), suggesting that these two flavonoids attenuate apoptosis at the mitochondrial level. Preincubation of cells with apigenin did not ameliorate the extent of caspase-3 cleavage in response to the toxic effects of H_2O_2.

DISCUSSION

There were five major findings from this study. 1) Different groups of flavonoids exhibited a scavenging activity against DPPH radical with different SC_{50} in the cell-free system; flavanols and flavonols were the most potent flavonoids, and flavanones were inactive in scavenging the radical. 2) The flavanol (-)epigallocatechin gallate and the flavonol quercetin at the nontoxic dose of 50 μmol/L prevented H_2O_2-induced injury and prolonged endothelial cell survival. 3) The flavones, luteolin and apigenin, intensified H_2O_2-induced endothelial apoptosis. 4) (-)Epigallocatechin gallate and quercetin restored expression of the antiapoptotic bcl-2 protein and increased expression of the proapoptotic bax protein in response to H_2O_2. 5) H_2O_2-induced caspase-3 cleavage in HUVEC was partially blocked by (-)epigallocatechin gallate and quercetin. These observations demonstrate that there are

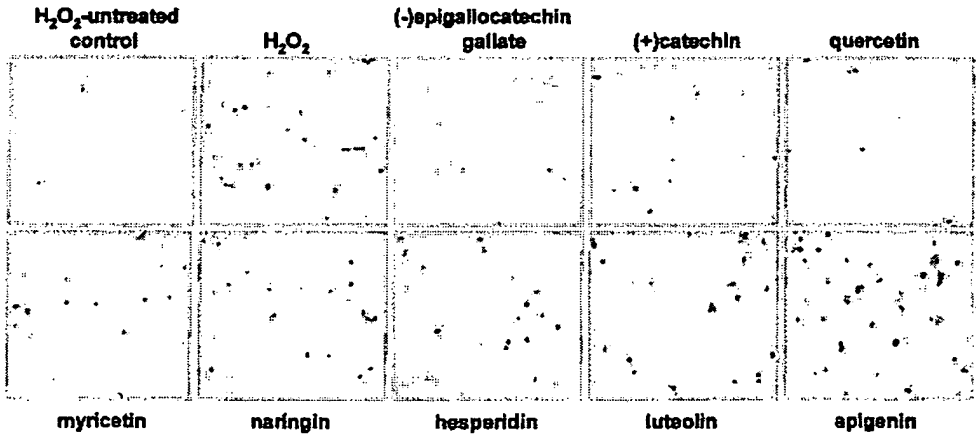

FIGURE 3 Representative microphotographs of terminal deoxynucleotidyl transferase-mediated dUTP nick end labeling–stained human umbilical vein endothelial cells (HUVEC) exposed to H_2O_2 and treated with 50 μmol/L flavonoids. These microphotographs are representative of 5 independent slides. Magnification: X200.

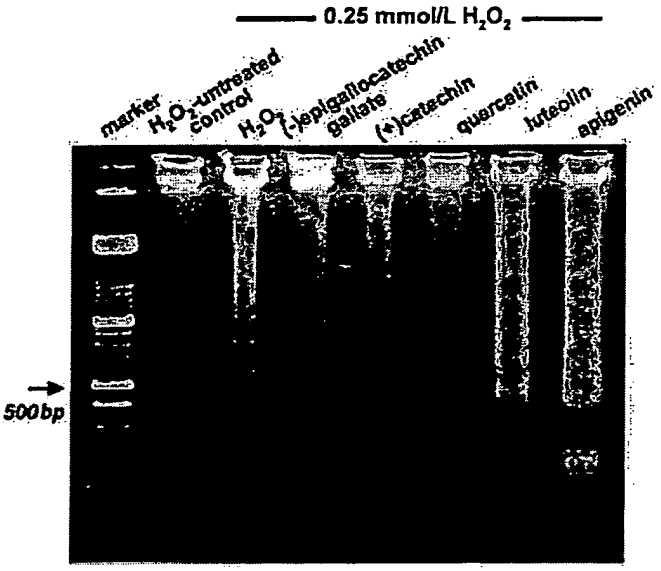

FIGURE 4 Genomic DNA gel electrophoresis of human umbilical vein endothelial cells (HUVEC) treated with H_2O_2 in the absence and presence of 50 μmol/L of selected flavonoids. Cells were incubated for 30 min without (lane 2) and with (lanes 3 to 8) 0.25 mmol/L H_2O_2. Lane 1 shows standard DNA markers. Five different experimental sets showed similar DNA run patterns.

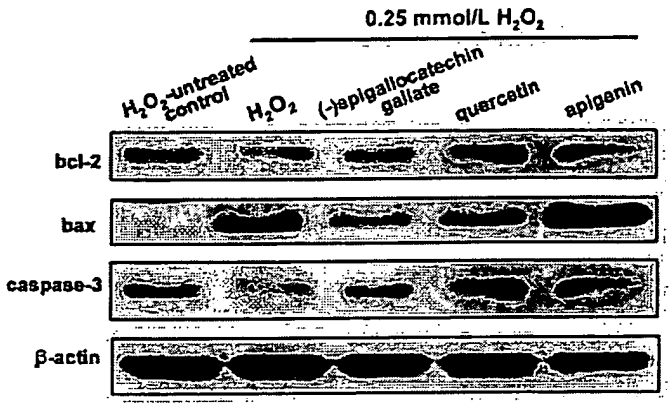

FIGURE 6 Bcl-2 and bax protein expression levels and caspase-3 cleavage in human umbilical vein endothelial cells (HUVEC) exposed to 0.25 mmol/L H_2O_2 for 30 min and incubated with flavonoids. The total HUVEC protein extract (100 μg) per lane was electrophoresed on 12 or 15% SDS-PAGE gels, followed by Western blot analysis with a primary antibody against bcl-2, bax or caspase-3. β-Actin protein was used as an internal control. Bands are representative of 5 independent experiments.

differences in the antiapoptotic activities of individual flavonoids, which appear to stem from their structure (Fig. 7).

Recent in vitro studies revealed that flavonoids may have considerable antioxidant activity in a wide range of chemical oxidation systems (16,17,20,21,35,36). In this study, some groups of flavonoids, e.g., flavanols and flavonols, exhibited a more powerful spontaneous antioxidant capacity scavenging the DPPH radical than the classic antioxidant L-ascorbic acid in the cell-free systems, whereas other flavonoids, especially apigenin, were not effective. Although we did not test a whole battery of flavonoids, we assume that there is a relationship between their structure and DPPH scavenging activity, as previously demonstrated (16,17,37,38).

Oxidative stress contributes to cellular injury after experimental ischemic reperfusion (5) and appears to be the common apoptotic mediator, most likely via lipid peroxidation (39). The literature has supported the role of ROS in apoptotic cell death. This study demonstrated that treatment of HUVEC with H_2O_2, a precursor of other ROS such as highly reactive hydroxyl radicals, leads to cell death via apoptotic processes. These findings are consistent with previous reports showing apoptotic death processes in various types of cells induced by H_2O_2 (34,40). Agents that inhibit production of ROS or enhance cellular antioxidant defenses can prevent apoptosis and protect cells from the damaging effects of oxygen radicals (4,9,10). Consistent with these reports, the flavanols and flavonols, in particular (-)epigallocatechin gallate and quercetin, had high antiapoptotic activities in the H_2O_2-treated vascular endothelial cells. In contrast, at nontoxic doses, the flavone-type flavonoids, luteolin and apigenin, had no antiapoptotic effects and intensified the apoptosis-like alterations, including nuclear condensation and DNA fragmentation. These results were in agreement with those obtained for DPPH scavenging activity, indicating that there is a major structural feature responsible for the antiapoptotic activity against reactive radicals (Fig. 7). In addition, the antiapoptotic activities of polyphenolic flavonoids proved to be diverse.

Dietary flavonoid supplementation reduces the incidence of myocardial infarction (12) and plasma LDL cholesterol concentration (11), and alleviates lipid peroxidation (41). Rodent feeding studies have supported the possibility that certain polyphenolics may have antioxidant functions in vivo (42,43). However, the underlying mechanisms for their cardio- and cytoprotective actions are still unknown. Their antioxidant actions in oxidant-induced endothelial apoptosis have been shown to be mediated through their H^+-donating properties (38). However, not all flavonoids tested in this study exhibited antiapoptotic activity in the H_2O_2-treated cells, suggesting that other mechanisms for cytoprotection against oxidant insults must be involved.

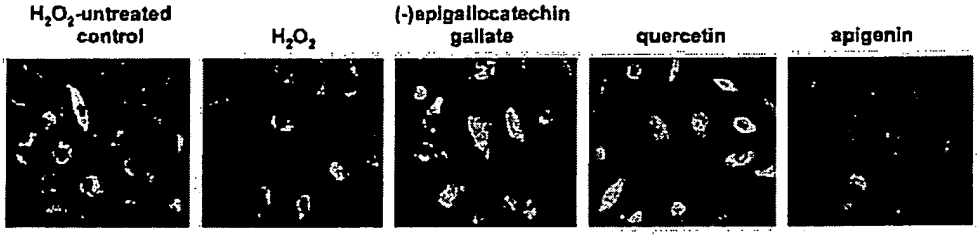

FIGURE 5 Expression of bcl-2 protein by immunocytochemical localization in human umbilical vein endothelial cells (HUVEC) incubated for 30 min with and without 0.25 mmol/L H_2O_2 in the absence and presence of 50 μmol/L of selected flavonoids. After fixation, antibody localization was detected with fluorescein isothiocyanate–conjugated goat anti-mouse immunoglobulin G. Magnification: X400.

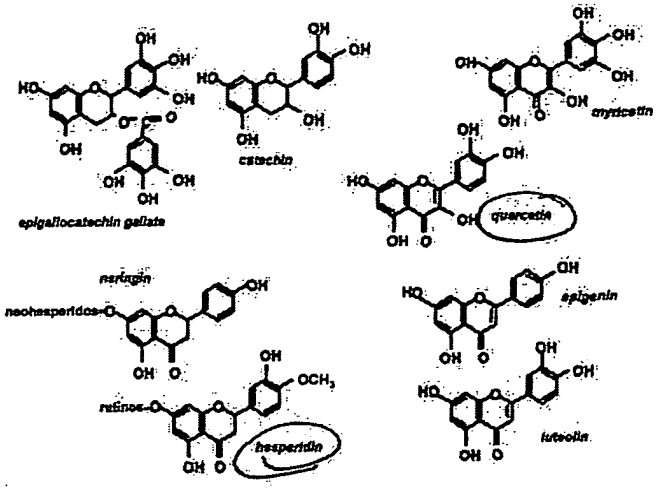

FIGURE 7 Chemical structure of the tested flavonoids.

(-)Epigallocatechin gallate and quercetin, with potent antiapoptotic actions, and apigenin, which was not antiapoptotic, were further tested for their effects on cascade events of the apoptotic pathway. It has been proposed that ROS down-regulate the antiapoptotic bcl-2 gene and up-regulate the pro-apoptotic bax gene, as shown in the present study. Bcl-2–expressing cells have been reported to have the enhanced antioxidant capacity that suppresses oxidative stress signals (44,45). In addition, enhancement of ROS has been reported to elicit translocation of cytosolic bax to mitochondria, and to activate bax to induce the release of cytochrome c from mitochondria, stimulating caspases (46). The H_2O_2-induced decrease in bcl-2 protein expression and the increase in bax expression were blocked in (-)epigallocatechin gallate- and quercetin-treated cells, providing compelling evidence in support of their potent antiapoptotic actions.

H_2O_2 strongly activated caspase-3, and the activation was partially blocked by (-)epigallocatechin gallate and almost completely by quercetin. The substantial difference between these flavonoids in inhibiting the activated caspase-3 appeared to be responsible for the difference in their antiapoptotic activities. (-)Epigallocatechin gallate and quercetin appeared to switch off the apoptotic death cascade by inhibiting the activation of caspase-3 and likely by enhancing the intrinsic cellular tolerance against apoptotic triggers. Conversely, the H_2O_2-activated caspase-3 was sustained in apigenin-treated cells that had no antiapoptotic ability. Thus, our findings suggest that the antiapoptotic flavonoids may function by acting selectively through various endothelial death signaling cascades. In addition, phytochemicals affect multiple signaling pathways that converge at the level of transcriptional regulation, i.e., mitogen-activated protein kinase–responsive pathways (47).

In summary, this endothelial cell model demonstrates that there are differences in antiapoptotic capacity among flavonoids, which appears to stem from their disparate chemical structures. Unlike flavones, the flavanol (-)epigallocatechin gallate and the flavonol quercetin protected the endothelium from oxidant-induced apoptosis. This antiapoptotic protection was possibly mediated at least in part by a mechanism linked to proapoptotic bax blockade and antiapoptotic bcl-2 activation. It is crucial to elucidate the precise sites of action of antiapoptotic flavonoids in the sequence of events that regulate oxidant-induced cell death and to further evaluate the potential of dietary flavonoids as cardio- and cytoprotective agents.

LITERATURE CITED

1. Jacobson, M. D., Weil, M. & Raff, M. C. (1997) Programmed cell death in animal development. Cell 88: 347–354.
2. Rathmell, J. C. & Thompson, C. B. (2002) Pathways of apoptosis in lymphocyte development, homeostasis, and disease. Cell 109: S97–S107.
3. Thompson, C. B. (1995) Apoptosis in the pathogenesis and treatment of disease. Science (Washington, DC) 267: 1456–1462.
4. Aoki, M., Nata, T., Morishita, R., Matsushita, H., Nakagami, H., Yamamoto, K., Yamazaki, K., Nakabayashi, M., Ogihara, T. & Kaneda, Y. (2001) Endothelial apoptosis induced by oxidative stress through activation of NF-κB: antiapoptotic effect of antioxidant agents on endothelial cells. Hypertension 38: 48–55.
5. Gottlieb, R. A., Burleson, K. O., Kloner, R. A., Babior, B. M. & Engler, R. L. (1994) Reperfusion injury induces apoptosis in rabbit cardiomyocytes. J. Clin. Investig. 94: 1621–1628.
6. Krown, K. A., Page, M. T., Nguyen, C., Zechner, D., Gutierrez, V., Comstock, K. L., Glembotski, C. C., Quintana, P. J. & Sabbadini, R. A. (1996) Tumor necrosis factor alpha-induced apoptosis in cardiac myocytes. Involvement of the sphingolipid signaling cascade in cardiac cell death. J. Clin. Investig. 98: 2854–2865.
7. Neuzil, J., Schroder, A., von Hundelshausen, P., Zernecke, A., Weber, T., Gellert, N. & Weber, C. (2001) Inhibition of inflammatory endothelial responses by a pathway involving caspase activation and p65 cleavage. Biochemistry 40: 4686–4692.
8. Gardner, A. M., Xu, F. H., Fady, C., Jacoby, F. J., Duffey, D. C., Tu, Y. & Lichtenstein, A. (1997) Apoptotic vs. nonapoptotic cytotoxicity induced by hydrogen peroxide. Free Radic. Biol. Med. 22: 73–83.
9. Lopez Farre, A. & Casado, S. (2001) Heart failure, redox alterations, and endothelial dysfunction. Hypertension 38: 1400–1405.
10. Rossig, L., Hoffmann, J., Hugel, B., Mallat, Z., Haase, A., Freyssinet, J. M., Tedgui, A., Aicher, A., Zeiher, A. M. & Dimmeler, S. (2001) Vitamin C inhibits endothelial cell apoptosis in congestive heart failure. Circulation 104: 2182–2187.
11. Arai, Y., Watanabe, S., Kimira, M., Shimoi, K., Mochizuki, R. & Kinae, N. (2000) Dietary intakes of flavonols, flavones and isoflavones by Japanese women and the inverse correlation between quercetin intake and plasma LDL cholesterol concentration. J. Nutr. 130: 2243–2250.
12. Geleijnse, J. M., Launer, L. J., Van der Kuip, D. A., Hofman, A. & Witteman, J. C. (2002) Inverse association of tea and flavonoid intakes with incident myocardial infarction: the Rotterdam Study. Am. J. Clin. Nutr. 75: 880–886.
13. Kris-Etherton, P. M. & Keen, C. L. (2002) Evidence that the antioxidant flavonoids in tea and cocoa are beneficial for cardiovascular health. Curr. Opin. Lipidol. 13: 41–49.
14. Borek, C. (2001) Antioxidant health effects of aged garlic extract. J. Nutr. 131: 1010S–1015S.
15. Arteel, G. E., Schroeder, P. & Sies, H. (2000) Reactions of peroxynitrite with cocoa procyanidin oligomers. J. Nutr. 130: 2100S–2104S.
16. Chen, J. W., Zhu, Z. Q., Hu, T. X. & Zhu, D. Y. (2002) Structure-activity relationship of natural flavonoids in hydroxyl radical-scavenging effects. Acta Pharmacol. Sin. 23: 667–672.
17. Dugas, A. J. Jr., Castaneda-Acosta, J., Bonin, G. C., Price, K. L., Fischer, N. H. & Winston, G. W. (2000) Evaluation of the total peroxyl radical-scavenging capacity of flavonoids: structure-activity relationships. J. Nat. Prod. 63: 327–331.
18. Gao, Z., Huang, K., Yang, X. & Xu, H. (1999) Free radical scavenging and antioxidant activities of flavonoids extracted from the radix of *Scutellaria baicalensis* Georgi. Biochim. Biophys. Acta 1472: 643–650.
19. Hanasaki, Y., Ogawa, S. & Fukui, S. (1994) The correlation between active oxygens scavenging and antioxidative effects of flavonoids. Free Radic. Biol. Med. 16: 845–850.
20. Sawa, T., Nakao, M. Akaike, T., Ono, K. & Maeda, H. (1999) Alkylperoxyl radical-scavenging activity of various flavonoids and other phenolic compounds: implications for the anti-tumor-promoter effect of vegetables. J. Agric. Food Chem. 47: 397–402.
21. Valcic, S., Muders, A., Jacobsen, N. E., Liebler, D. C. & Timmermann, B. N. (1999) Antioxidant chemistry of green tea. Identification of products of the reaction of (-)-epigallocatechin gallate with peroxyl radicals. Chem. Res. Toxicol. 12: 382–386.
22. Bito, T., Roy, S., Sen, C. K., Shirakawa, T., Gotoh, A., Ueda, M., Ichihashi, M. & Packer, L. (2002) Flavonoids differentially regulate IFN gamma-induced ICAM-1 expression in human keratinocytes: molecular mechanisms of action. FEBS Lett. 520: 145–152.
23. Sartor, L., Pezzato, E., Dell'Aica, I., Caniato, R., Biggin, S. & Garbisa, S. (2002) Inhibition of matrix-proteases by flavonoids: chemical insights for anti-inflammatory and anti-invasion drug design. Biochem. Pharmacol. 64: 229–237.
24. Middleton, E., Jr., Kandaswami, C. & Theoharides, T. C. (2000) The effects of plant flavonoids on mammalian cells: implications for inflammation, heart disease, and cancer. Pharmacol. Rev. 52: 673–751.
25. Fuhrman, B. & Aviram, M. (2001) Flavonoids protect LDL from oxidation and attenuate atherosclerosis. Curr. Opin. Lipidol. 12: 41–48.

26. Anderson, J. J. & Garner, S. C. (1998) Phytoestrogens and bone. Baillieres Clin. Endocrinol. Metab. 12: 543–557.

27. Blois, M. S. (1958) Antioxidant determinations by the use of a stable free radical. Nature (Lond.) 181: 1199–1200.

28. Jaffe, E. A., Nachman, R. L., Becker, C. G. & Minick, C. R. (1973) Culture of human endothelial cells derived from umbilical veins. Identification by morphologic and immunologic criteria. J. Clin. Investig. 52: 2745–2756.

29. Voyta, J. C., Via, D. P., Butterfield, C. E. & Zetter, B. R. (1984) Identification and isolation of endothelial cells based on their increased uptake of acetyl-low density lipoprotein. J. Cell. Biol. 99: 2034–2040.

30. Denizot, F. & Lang, R. (1986) Rapid colorimetric assay for cell growth and survival. Modification to the tetrazolium dye procedure giving improved sensitivity and reliability. J. Immunol. Methods 89: 271–277.

31. Wyllie, A. H., Morris, R. G., Smith, A. L. & Dunlop, D. (1984) Chromatin cleavage in apoptosis: association with condensed chromatin morphology and dependence on macromolecular synthesis. J. Pathol. 142: 67–77.

32. Gavrieli, Y., Sherman, Y. & Ben-Sasson, S. A. (1992) Identification of programmed cell death *in situ* via specific labeling of nuclear DNA fragmentation. J. Cell. Biol. 119: 493–501.

33. Arends, M. J., Moris, R. G. & Wyllie, A. H. (1990) Apoptosis: role of the endonuclease. Am. J. Pathol. 136: 593–608.

34. Kang, Y. H., Chung, S. J., Kang, I. J., Park, J. H. Y. & Bünger, R. (2001) Mitochondrial pyruvate prevents hydrogen peroxide-induced apoptosis in vascular endothelial cells. Mol. Cell. Biochem. 216: 37–46.

35. Kashima, M. (1999) Effects of catechins on superoxide and hydroxyl radical. Chem. Pharm. Bull. 47: 279–283.

36. Pannala, A. S., Rice-Evans, C. A., Halliwell, B. & Singh, S. (1997) Inhibition of peroxynitrite-mediated tyrosine nitration by catechin polyphenols. Biochem. Biophys. Res. Commun. 232: 164–168.

37. Cos, P., Rajan, P., Vedernikova, I., Calomme, M., Pieters, L., Vlietinck, A. J., Augustyns, K., Haemers, A. & Vanden Berghe, D. (2002) In vitro antioxidant profile of phenolic acid derivatives. Free Radic. Res. 36: 711–716.

38. Rice-Evans, C. A., Miller, N. J. & Paganga, G. (1996) Structure-antioxidant activity relationships of flavonoids and phenolic acids. Free Radic. Biol. Med. 20: 933–956.

39. Buttke, T. M. & Sandstrom, P. A. (1994) Oxidative stress as a mediator of apoptosis. Immunol. Today 15: 7–10.

40. Spencer, J. P. E., Schroeter, H., Kuhnle, G., Srai, S. K. S., Tyrrell, R. M., Hahn, U. & Rice-Evans, C. (2001) Epicatechin and its *in vivo* metabolite, 3′-*O*-methyl epicatechin, protect human fibroblasts from oxidative-stress-induced cell death involving caspase-3 activation. Biochem. J. 354: 493–500.

41. Freese, R., Basu, S., Hietanen, E., Nair, J., Nakachi, K., Bartsch, H. & Mutanen, M. (1999) Green tea extract decreases plasma malondialdehyde concentration but does not affect other indicators of oxidative stress, nitric oxide production, or hemostatic factors during a high-linoleic acid diet in healthy females. Eur. J. Nutr. 38: 149–157.

42. Funabiki, R., Takeshita, K., Miura, Y., Shibasato, M. & Nagasawa, T. (1999) Dietary supplement of G-rutin reduces oxidative damage in the rodent model. J. Agric. Food Chem. 47: 1078–1082.

43. Giovannini, L., Migliori, M., Longoni, B. M., Das, D. K., Bertelli, A. A., Panichi, V., Filippi, C. & Bertelli, A. (2001) Resveratrol, a polyphenol found in wine, reduces ischemia reperfusion injury in rat kidneys. J. Cardiovasc. Pharmacol. 37: 262–270.

44. Hockenbery, D. M., Olival, Z. N., Yin, X.-M., Milliman, C. I. & Korsmeyer, S. J. (1993) *Bcl-2* functions in an antioxidant pathway to prevent apoptosis. Cell 75: 241–251.

45. Voehringer, D. W. & Meyn, R. E. (2000) Redox aspects of bcl-2 function. Antioxid. Redox Signal. 2: 537–550.

46. Cai, J. & Jones, D. P. (1998) Superoxide in apoptosis. Mitochondrial generation triggered by cytochrome c loss. J. Biol. Chem. 273: 11401–11404.

47. Frigo, D. E., Duong, B. N., Melnik, L. I., Schief, L. S., Collins-Burow, B. M., Pace, D. K., McLachlan, J. A. & Burow, M. E. (2002) Flavonoid phytochemicals regulate activator protein-1 signal transduction pathways in endometrial and kidney stable cell lines. J. Nutr. 132: 1848–1853.

0090-9556/07/3507-1203–1208$20.00
DRUG METABOLISM AND DISPOSITION
Copyright © 2007 by The American Society for Pharmacology and Experimental Therapeutics
DMD 35:1203–1208, 2007

Vol. 35, No. 7
13904/3223202
Printed in U.S.A.

Esterase Inhibition by Grapefruit Juice Flavonoids Leading to a New Drug Interaction

Ping Li, Patrick S. Callery, Liang-Shang Gan, and Suresh K. Balani

Drug Metabolism and Pharmacokinetics, Drug Safety and Disposition, Millennium Pharmaceuticals, Inc., Cambridge, Massachusetts (P.L., L.-S.G., S.K.B.); and Department of Basic Pharmaceutical Sciences, School of Pharmacy, West Virginia University, Morgantown, West Virginia (P.L., P.S.C.)

Received November 14, 2006; accepted April 19, 2007

ABSTRACT:

Our previous studies described a newly identified potential of grapefruit juice (GFJ) in mediating pharmacokinetic drug interactions due to its capability of esterase inhibition. The current study identifies the active components in GFJ responsible for its esterase-inhibitory effect. The esterase-inhibitory potential of 10 constitutive flavonoids and furanocoumarins toward *p*-nitrophenylacetate (PNPA) hydrolysis was investigated. The furanocoumarins bergamottin, 6′,7′-dihydroxybergamottin, and bergapten, and the glycoside flavonoids naringin and hesperidin, at concentrations found in GFJ or higher, did not inhibit the hydrolysis of PNPA by purified porcine esterase and human liver microsomes. However, the flavonoid aglycones morin, galangin, kaempferol, quercetin, and naringenin showed appreciable inhibition of PNPA hydrolysis in purified porcine esterase, and human and rat liver systems. In Caco-2 cells, demonstrated to contain minimal CYP3A activity, the permeability coefficient of the prodrugs lovastatin and enalapril was increased in the presence of the active flavonoids kaempferol and naringenin, consistent with inhibition of esterase activity. In rats, oral coadministration of kaempferol and naringenin with these prodrugs led to significant increases in plasma exposure to the active acids. In addition, in portal vein-cannulated rats, coadministration of lovastatin with kaempferol (10 mg/kg) led to a 154% and a 113% increase in the portal plasma exposure to the prodrug and active acid, respectively, compared with coadministration with water. The contribution of CYP3A inhibition was demonstrated to be minimal. Overall, a series of flavonoids present in GFJ are identified as esterase inhibitors, of which kaempferol and naringenin are shown to mediate pharmacokinetic drug interaction with the prodrugs lovastatin and enalapril due to their capability of esterase inhibition.

Since the first report of the GFJ effect on the oral bioavailability of felodipine (Bailey et al., 1989, 1991), many studies to identify the active components responsible for the GFJ effects have been reported (Bailey et al., 1993; Edwards et al., 1996; Fukuda et al., 1997; Schmiedlin-Ren et al., 1997; He et al., 1998; Guo et al., 2000; Ho et al., 2001). GFJ composition varies from variety to variety and from lot to lot and also depends on the preparation method (De Castro et al., 2006). In all cases, the majority of the constituents are flavonoids (Ho et al., 2000). Naringin, a predominant constituent in GFJ, is present in concentrations up to 2000 μM (Ross et al., 2000). Even flavonoids of relatively low abundance such as quercetin exist in the 20 μM range. Bergamottin and 6′,7′-dihydroxybergamottin (6′,7′-DHB), the most abundant furanocoumarin derivatives and another well studied GFJ constituent, are present in concentrations up to 40 μM (Edwards et al., 1996). Although many bioflavonoids inhibited CYP3A in vitro (Ho et al., 2001), in vivo, naringin by itself, at concentrations found in GFJ, was not capable of producing a clinical drug interaction such as that seen with grapefruit juice (Bailey et al., 1998). Several furanocoumarins in grapefruit juice are effective in vitro CYP3A inhibitors and are currently suggested to be clinically active constituents (Schmiedlin-Ren et al., 1997; He et al., 1998).

Our previous study (Li et al., 2007) demonstrated that GFJ inhibits esterase activity and mediates pharmacokinetic interaction with the ester prodrugs lovastatin and enalapril. It is important to identify the active components responsible for this new esterase-mediated GFJ effect in vivo. Several classical esterase inhibitors are known, including diethyl *p*-nitrophenyl phosphate and bis-*p*-nitrophenylphosphate (BNPP). However, the extreme toxicity of these compounds precludes their clinical use. Recently, a series of synthesized benzene sulfonamides and the aromatic dione family were identified as selective inhibitors of carboxylesterases (Wadkins et al., 2004, 2005). Likewise, flavoring ester mixtures in strawberry juice were also reported to interact with the prodrug tenofovir, leading to enhanced permeability across Caco-2 (van Gelder et al., 2002). Our recent report (Li et al., 2007) demonstrated that GFJ decreased lovastatin and enalapril hydrolysis in the gut and thereby markedly increased metabolic stability and permeability of esters, leading to the enhancement of exposure to lovastatin acid and enalaprilat in rats. In the current report, the esterase inhibition potential of 10 grapefruit juice components toward

Article, publication date, and citation information can be found at http://dmd.aspetjournals.org.
doi:10.1124/dmd.106.013904.

ABBREVIATIONS: GFJ, grapefruit juice; AUC, area under the curve; BNPP, bis-(*p*-nitrophenyl phosphate); PMSF, phenylmethylsulfonyl fluoride; PNPA, *p*-nitrophenylacetate; 6′,7′-DHB, 6′,7′-dihydroxybergamottin; LC/MS/MS, liquid chromatography-tandem mass spectrometry; Pgp, P-glycoprotein; GF120918, *N*-(4-[2-(1,2,3,4-tetrahydro-6,7-dimethoxy-2-isoquinolinyl)ethyl]-phenyl)-9,10-dihydro-5-methoxy-9-oxo-4-acridine carboxamide; PK, pharmacokinetic; A-to-B, apical-to-basal.

p-nitrophenylacetate (PNPA) hydrolysis as well as the effect of 2 selected components on the esterase-mediated changes in the permeability in in vitro systems, and in in vivo rat exposure to active acids of enalapril and lovastatin upon coadministration are described.

Materials and Methods

Materials. Enalapril, lovastatin, PNPA, *p*-nitrophenol, phenylmethylsulfonyl fluoride (PMSF), BNPP, bergapten, kaempferol, quercetin, morin, galangin, naringenin, naringin, and hesperidin were purchased from Sigma (St. Louis, MO). Bergamottin and 6′,7′-DHB were purchased from BD Gentest (Woburn, MA); enalaprilat and lovastatin hydroxy acid were purchased from Toronto Research Chemicals Inc. (North York, ON, Canada). Human liver microsomes (pool of 50) were purchased from XenoTech, LLC (Lenexa, KS), and purified porcine esterase was purchased from Sigma. Caco-2 cells were obtained from The American Type Culture Collection (Manassas, VA).

Inhibition of Esterase Activity in Purified Porcine Esterase and Human Liver Microsomes. Purified porcine liver esterase (5 mU/ml) or human liver microsomes (0.1 mg/ml) in 0.1 M potassium phosphate buffer pH 7.4 were incubated at 37°C with PNPA (667 μM) and one of the 10 GFJ components of 10 different concentrations: bergamottin (0~100 μM), bergapten (0~100 μM), 6′,7′-DHB (0~100 μM), kaempferol (0~50 μM), quercetin (0~50 μM), morin (0~50 μM), galangin (0~50 μM), naringenin (0~200 μM), hesperidin (0~200 μM), and naringin (0~1000 μM). The highest concentration of each component used for esterase inhibition evaluation varied based on their solubility in incubation buffer and their concentration found in GFJ. The formation of the product, *para*-nitrophenol, was monitored spectrophotometrically at 405 nm at 2 min.

Inhibitory Effect on Esterase Activity in Rat Liver Microsomes or S9 Fractions. Rat liver microsomes (2.0 mg/ml) or S9 (2.5 mg/ml) in 0.1 M potassium phosphate buffer pH 7.4 were incubated at 37°C with enalapril (5 μM) (using microsomes) or lovastatin (5 μM) (using S9) in the presence or absence of kaempferol (100 μM), naringenin (100 μM), BNPP (100 μM), or PMSF (1000 μM). The reactions were terminated by adding an equal volume of acetonitrile containing 0.5 μM carbutamide (internal standard) after 10 min of incubation. The samples were kept in a refrigerator (4°C) for 30 min and then centrifuged at 3000*g* for 10 min. The concentrations of enalaprilat or lovastatin acid in the supernatants were analyzed with LC/MS/MS.

Permeability in Caco-2 Membrane. Caco-2 cell cultures were prepared as described previously (Xia et al., 2005). Single directional transport studies were performed at 37°C in air. Before each experiment, the confluent cell monolayer on Transwell inserts was washed and equilibrated for 30 min with transport medium (Hanks' balanced salt solution containing 10 mM HEPES and 10 mM glucose pH 7.4). The experiment (n = 4) was initiated by adding a solution of lovastatin (20 μM final concentration) in the transport medium at pH 7.0 or enalapril (20 μM final concentration) in the transport medium at pH 6.0 (lower pH to facilitate PEPT1-mediated transport), containing various amounts of kaempferol or naringenin (50 or 250 μM final concentration), to the apical compartment. To evaluate the Pgp effect on lovastatin permeability, GF120918 (2 μM final concentrations in the incubation) was added into lovastatin stock solution on the donor side and buffer on the receiver side. At 15, 30, 45, and 60 min, aliquots were withdrawn from the basolateral side and replaced immediately with an equal amount of fresh transport medium, except at the 60-min time point (the end of the incubation). After the permeability studies described in the previous section, transendothelial electrical resistance values were measured again to assure the integrity of the cells. The cells were washed three times with cold transport medium and then were lysed with 1% acetic acid in water. The cell lysates were extracted with acetonitrile containing carbutamide as internal standard and centrifuged at 3000*g* for 10 min. The supernatants were collected and analyzed using LC/MS/MS.

Pharmacokinetics Studies. Pharmacokinetics experiments with enalapril and lovastatin were performed in male Sprague-Dawley rats (Hilltop Laboratory Animals, Inc., Scottdale, PA), weighing 280 to 350 g, that were implanted with either a jugular vein cannula or both jugular and portal vein cannulas. Animals were fasted overnight and for the duration of the study. Water was provided ad libitum. All experiments with rats were performed in accordance with the Institutional Animal Care and Use Committee guidelines and approved by the Committee on Animal Research, Millennium Pharmaceuticals Inc.

For systemic exposure studies, jugular vein-cannulated rats (n = 3) were orally dosed by gavage with enalapril and lovastatin (10 mg/kg, 10 ml/kg) in 1) water, 2) kaempferol (2 and 10 mg/kg); and 3) naringenin (2 and 10 mg/kg). Venous blood samples (0.3 ml) were collected from jugular vein catheters into heparin tubes containing 3 μl of 200 mM PMSF and 5 μl of acetic acid (6:4 diluted with water) predose and at 0.25, 0.5, 1, 2, 4, 6, 8, and 24 h postdose. Samples were centrifuged, and plasma samples were collected and frozen at −80°C until analyzed.

For portal exposure studies, portal vein-cannulated rats (n = 4) were orally dosed by gavage with lovastatin (10 mg/kg, 10 ml/kg) in 1) water or 2) kaempferol (10 mg/kg). Portal blood samples (0.3 ml) were collected from portal vein-cannulated rats into heparin tubes containing 3 μl of 200 mM PMSF and 5 μl of acetic acid (6:4 diluted with water) predose and at 0.25, 0.5, 1, 2, 4, 6, 8 and 24 h postdose. Samples were centrifuged, and plasma samples were collected and frozen at −80°C until analyzed.

LC/MS/MS Analysis. In vivo plasma samples were protein-precipitated and analyzed with an LC/MS/MS method. Blank plasma, in which esterase was inactivated with 1% acetic acid and 2 mM PMSF, was used to construct plasma standard curves. In general, to 1 volume of plasma was added 3 volumes of acetonitrile containing carbutamide as the internal standard. Samples were vortexed and then centrifuged for 15 min at 3000*g*. Half of the supernatant was dried down under nitrogen and reconstituted with 150 μl of 5% acetonitrile in 0.1% formic acid. The LC/MS/MS system consisted of a binary high performance liquid chromatography pump (1100; Agilent Technologies, Palo Alto, CA), an HTS PAL autosampler (LEAP Technologies, Carrboro, NC), and a triple-quadrupole mass spectrometer (API-4000; Applied Biosystems, Foster City, CA). Separation was performed on a YMC-ODS-AQ C18 column (30 mm × 2.0 mm; Waters, Milford, MA) using mixtures of formic acid (0.1%) in water and acetonitrile as a mobile phase. The mass spectrometer was operated in the multiple reaction monitoring mode using positive ion electrospray ionization. Multiple reaction monitoring was set at *m/z* 405.3 → 285.3 for lovastatin, 423.3 → 303.4 for lovastatin acid, 421.4 → 283.4 for 6′β-hydroxylovastatin, 377.1 → 233.9 for enalapril, and 349.3 → 206.4 for enalaprilat. The quantification limit for enalapril, enalaprilat, lovastatin, and lovastatin acid was generally 2 nM.

Data Analysis. Percentage inhibition of PNPA hydrolysis for each inhibitor was calculated as the ratio of OD at each concentration of inhibitor with respect to that in the absence of the inhibitor, and the percentages were plotted against the concentrations of each tested inhibitor using Prism software (GraphPad Software Inc., San Diego, CA). The sigmoidal dose-response (variable slope) model was used to determine the concentration that gave 50% inhibition (IC_{50}). The IC_{50} was calculated using the equation Y = minimum activity + (maximum activity − minimum activity)/$(1 + 10^{((\log IC_{50} - X) \cdot \text{Hill slope})})$, where X is the logarithm of concentration and Y is the percentage activity.

PK parameters were calculated by noncompartmental analysis using WinNonlin software version 5.1 (Pharsight, Mountain View, CA). Statistical analysis was performed using Student's t test. Apparent permeability (P_{app}, cm/s × 10^{-6}) was calculated using the equation $P_{app} = (dQ/dt)/(A \cdot C_0)$, where dQ/dt = total amount transported in the recipient chamber per unit time (e.g., nmol/s), A = surface area (cm^2; in our studies A = 0.33 cm^2), and C_0 = initial donor concentration (e.g., nmol/ml).

Results

Effect of GFJ Components on Purified Porcine Esterase and Human Liver Microsomal Hydrolase Activity. Inhibitory activity of GFJ components toward esterase activity varied widely. Bergamottin, 6′,7′-DHB, and bergapten (each at 100 μM), hesperidin at 200 μM, and naringin at 1000 μM did not show appreciable inhibition of the hydrolysis of PNPA by porcine liver esterase. However, morin, galangin, kaempferol, quercetin, and naringenin showed inhibitory effects. Estimates of IC_{50} were 1.8 μM for morin, 2.8 μM for galangin, 5.1 μM for kaempferol, 5.9 μM for quercetin, and 110 μM for naringenin (Table 1). Likewise, in human liver microsomes, bergamottin, 6′,7′-DHB, bergapten, naringin, and hesperidin did not

DMD DRUG METABOLISM AND DISPOSITION aspet

TABLE 1

Inhibitory effect of GFJ components toward PNPA hydrolysis by purified porcine esterase and human liver microsomes

Inhibitor	Porcine Esterase IC_{50}	Human Liver Microsomes IC_{50}
	μM	
Kaempferol	5.1	62
Quercetin	5.9	43
Morin	1.8	80
Galangin	2.8	81
Naringenin	110	30
Hesperidin	>200	>200
Naringin	>1000	>1000
Bergamottin	>100	>100
6',7'-DHB	>100	>100
Bergapten	>100	>100

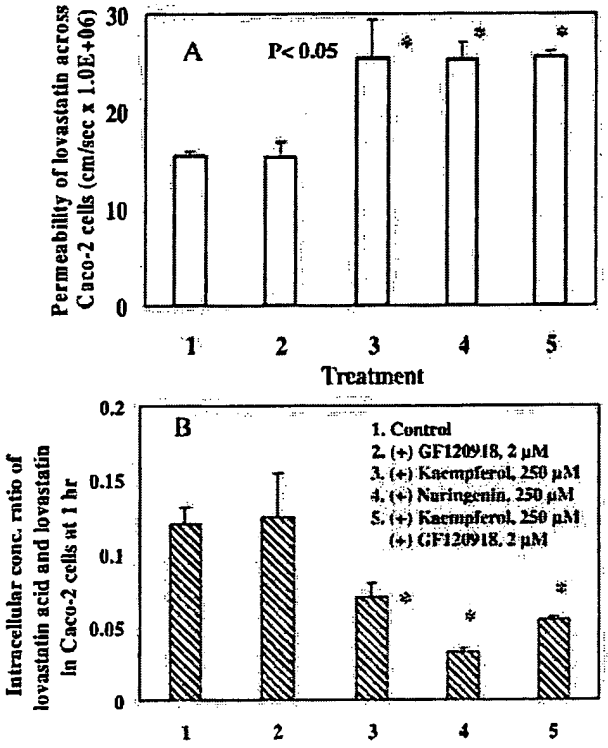

FIG. 1. Effect of kaempferol and naringenin on lovastatin A→B permeability across Caco-2 membrane (A) and ratio of lovastatin acid and lovastatin in Caco-2 cells at 1 h (B).

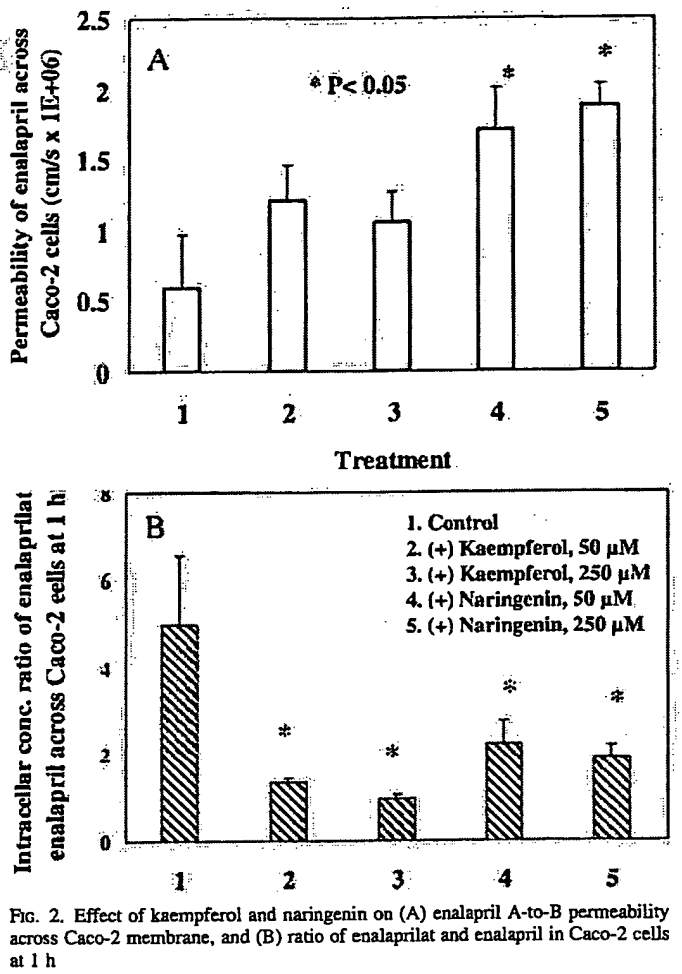

FIG. 2. Effect of kaempferol and naringenin on (A) enalapril A-to-B permeability across Caco-2 membrane, and (B) ratio of enalaprilat and enalapril in Caco-2 cells at 1 h

appreciably inhibit the hydrolysis of PNPA. Estimates of IC_{50} for human liver microsomes were 80 μM for morin, 81 μM for galangin, 62 μM for kaempferol, 43 μM for quercetin, and 30 μM for naringenin.

Effect of Kaempferol and Naringenin on A-to-B Permeability in Caco-2 Cells. The permeability of lovastatin was not altered by GF120918 alone (−0.5%), and was increased by 65, 64, and 66% by kaempferol (250 μM), naringenin (250 μM), and the mixture of kaempferol (250 μM) and GF120918 (2 μM; Fig. 1A). In Caco-2 cells, at 1 h, the intracellularly trapped lovastatin was not significantly altered, with the respective values of 117, 95.8, 105, and 116% of the control (1316 pmol), whereas the trapped amount of lovastatin acid was unaffected by GF120918 alone (120%) and decreased to 54.5, 28.6, and 51.6% by kaempferol, naringenin, and a mixture of kaempferol and GF120918 relative to the control (161 pmol). The overall ratios of lovastatin acid to lovastatin in Caco-2 cells were decreased and are shown in Fig. 1B. The permeability of enalapril was increased by 106, 79.4, 188, and 219% with kaempferol (50 and 250 μM) and naringenin (50 and 250 μM), respectively (Fig. 2A). The corresponding intracellularly trapped enalapril in Caco-2 cells at 1 h was increased by 67.3, 69.1, and 26.2%, and decreased by 11% relative to the control (9.9 pmol); and enalaprilat was decreased to 54.5, 36.8, 57.8, and 39.7% relative to the control (41 pmol). The overall ratios of enalaprilat to enalapril were decreased and are shown in Fig. 2B. The amount of lovastatin acid and enalaprilat on the donor side, at the end of the incubation, was very low and was not affected by kaempferol and naringenin.

Effect of Kaempferol and Naringenin on Enalapril and Lovastatin Hydrolysis in Rat Liver Microsomes or S9 Fractions. The percentage of lovastatin hydrolyzed in rat liver S9 (8.8 pmol/min/mg) was reduced to 55, 72, 54, and 24% of the control by kaempferol, naringenin, BNPP, and PMSF, respectively (Fig. 3A). Enalapril hydrolysis in rat liver microsomes (62.8 pmol/min/mg) was reduced to 29, 66, 19, and 1% of the control by kaempferol, naringenin, BNPP, and PMSF, respectively (Fig. 3B).

Effect of Kaempferol and Naringenin on Oral Pharmacokinetics of Lovastatin Acid and Enalaprilat in Rats. The plasma concentration-time profiles of lovastatin acid and enalaprilat in rats following oral coadministration of lovastatin and enalapril (10 mg/kg) with water, kaempferol (2 and 10 mg/kg), and naringenin (2 and 10 mg/kg) are shown in Figs. 4 and 5. The PK data are shown in Table 2.

Effect of Kaempferol on the Portal Plasma Pharmacokinetics of Lovastatin. The portal vein plasma concentration-time profiles of

DRUG METABOLISM AND DISPOSITION DMD aspet

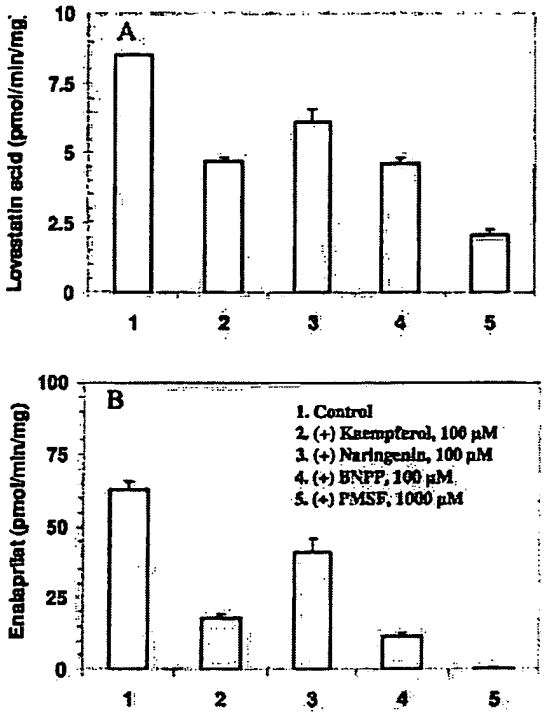

FIG. 3. Inhibition of hydrolysis of lovastatin (5 μM) in rat liver S9 fraction (A) and enalapril (5 μM) in rat liver microsomes (B) by kaempferol, naringenin, BNPP, and PMSF.

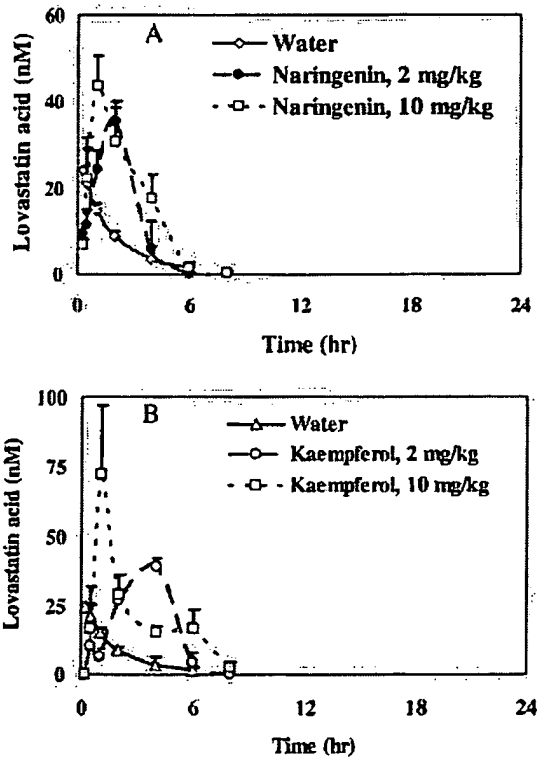

FIG. 4. Plasma concentration-time profiles of lovastatin acid following oral administration of lovastatin at 10 mg/kg with water (A) or naringenin (2 and 10 mg/kg) with water or kaempferol (2 and 10 mg/kg) (B).

lovastatin, lovastatin acid, and the major oxidative product, 6′β-hydroxylovastatin, following oral coadministration of lovastatin (10 mg/kg) to rats with water or kaempferol (10 mg/kg) are shown in Fig.

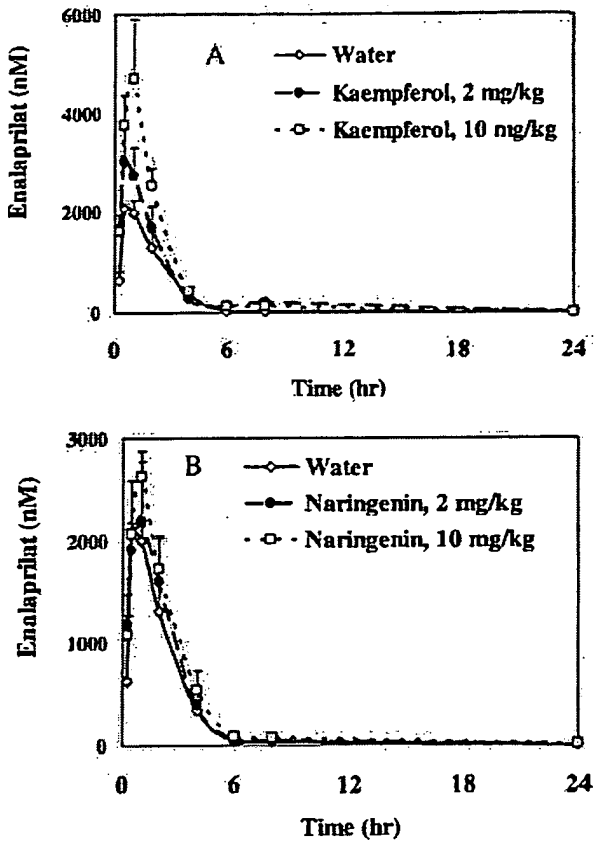

FIG. 5. Plasma concentration-time profiles of enalaprilat following oral administration of enalapril at 10 mg/kg with water (A) or naringenin (2 and 10 mg/kg) with water or kaempferol (2 and 10 mg/kg) (B).

6. The 6′β-hydroxylovastatin was identified by LC/MS/MS spectral comparison with the published data (Halpin et al., 1993) and quantitated in plasma using lovastatin standard curves. The portal plasma PK parameters are shown in Table 3. The AUC ratio of 6′β-hydroxylovastatin and lovastatin was 0.064 and 0.078 in rats upon coadministration of lovastatin with water and kaempferol, respectively.

Discussion

Inhibition of Esterase Activity in Purified Porcine Esterase and Human Liver Microsomes. The 10 grapefruit components investigated in this study belong to two major and widely known classes, flavonoids (aglycones and glycosides) and furanocoumarins. In the earlier years, grapefruit flavonoids were extensively studied for their CYP3A inhibition potential for understanding the GFJ effect on oral bioavailability of CYP3A substrates. Although these flavonoids inhibited CYP3A4 in vitro, they did not reproduce the grapefruit juice effect when administered orally (Bailey et al., 1993; Rashid et al., 1993). Currently, it is believed that the furanocoumarins, bergamottin and 6′,7′-DHB, in GFJ are responsible for the GFJ interaction by competitive and mechanism-based inhibition of CYP3A in the small intestine. These two potent CYP3A inhibitors, in the current study, were found to be devoid of esterase-inhibitory activity in purified porcine esterase and human liver microsomes at 100 μM, a concentration higher than that found in GFJ. Some of the flavonoids, on the other hand, were found to have esterase-inhibitory activity. The effect of flavonoids in aglycone form on carboxylesterases is distinguishable from that of flavonoids in glycoside form. Naringin and hesperidin, the two glycosidic flavonoids, did not inhibit PNPA hydrolysis at

DMD DRUG METABOLISM AND DISPOSITION aspet

TABLE 2

Effect of naringenin (2 and 10 mg/kg) and kaempferol (2 and 10 mg/kg) on PK parameters of enalaprilat and lovastatin acid following oral coadministration with enalapril and lovastatin (10 mg/kg) to rats

Data are mean values ± standard deviation (n = 3).

Coadministration	Enalaprilat			Lovastatin Acid		
	$AUC_{0-6\ h}$	T_{max}	C_{max}	$AUC_{0-6\ h}$	T_{max}	C_{max}
	nM · h	*h*	*nM*	*nM · h*	*h*	*nM*
Water	5494 ± 2309	0.66 ± 0.28	2163 ± 932	32.5 ± 1.1	0.4 ± 0.2	28.5 ± 12.7
Naringenin 2 mg/kg	6473 ± 3162	0.83 ± 0.29	2213 ± 882	84.1 ± 11.7*	1.7 ± 0.6	38.0 ± 6.9
Naringenin 10 mg/kg	7597 ± 2190	1.0 ± 0.0	2620 ± 436	126 ± 31.2*	1.3 ± 0.6	48.9 ± 8.2
Kaempferol 2 mg/kg	8814 ± 3279	0.5 ± 0.0	3033 ± 1161	88.1 ± 16.5*	1.6 ± 0.5	41.6 ± 5.2
Kaempferol 10 mg/kg	11498 ± 3386*	0.8 ± 0.2	4830 ± 1939	112 ± 11.1*	0.4 ± 0.14	72.0 ± 42.9

* Statistically significant difference ($P < 0.05$).

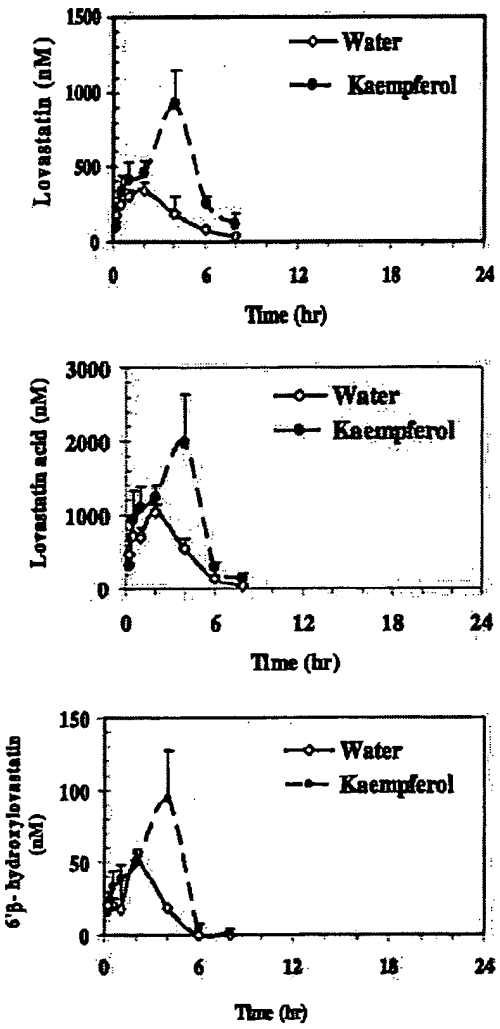

FIG. 6. Portal plasma concentration-time profiles of lovastatin (top), lovastatin acid (middle), and 6'β-hydroxylovastatin (bottom) following oral administration of lovastatin (10 mg/kg) with water or kaempferol (10 mg/kg). 6'β-Hydroxylovastatin was quantitated in plasma using lovastatin standard curves.

concentrations found in GFJ. However, the five flavonoids morin, galangin, kaempferol, quercetin, and naringenin, aglycone forms, markedly inhibited PNPA hydrolysis by purified porcine esterase, with IC_{50} values in the low micromolar range, 1.8 to 110 μM, and by human liver microsomes with IC_{50} values in the range of 30 to 81 μM. The higher values with human liver microsomes are believed to be due to a higher protein concentration (lower free concentrations) than that in purified enzyme, and do not necessarily reflect species differences. Nevertheless, these data show that there is a potential of esterase inhibition by these flavonoids in vivo in humans. The combined effects of flavonoids could contribute significantly to the GFJ effects on the pharmacokinetics of ester prodrugs. The effect of kaempferol and naringenin, two of the major and potent esterase-inhibitory flavonoids in GFJ, on the permeability of enalapril and lovastatin in the Caco-2 model, hydrolysis in the rat liver system, and pharmacokinetics in rats were examined. Kaempferol was reported to inhibit CYP3A and Pgp in vitro (Jignesh et al., 2004). Caco-2 cells used in our study were determined to show Pgp and esterase activities, but only a minor CYP3A activity (data not shown). Thus, in this Caco-2 model, the effect of kaempferol on lovastatin could mainly be due to Pgp and/or esterase. Kaempferol and naringenin led to enhancement of the A-to-B permeability of lovastatin and enalapril (Figs. 1A and 2A). GF120918, a Pgp and BCRP inhibitor (Xia et al., 2005), failed to significantly alter lovastatin permeability, suggesting that the contribution of Pgp to the permeability of lovastatin was negligible. Thus, it is mainly the esterase inhibition attribute of kaempferol and naringenin that led to the higher permeability of lovastatin and enalapril. As expected, in these experiments the intracellularly trapped lovastatin acid and enalaprilat were reduced by kaempferol and naringenin, as indicated by decreases in the ratios of lovastatin acid to lovastatin to 59, 27, and 45% by kaempferol, naringenin, and a mixture of kaempferol and GF120918 (Fig. 1B), and by decreases in the ratios of enalaprilat to enalapril to 27, 19, 44, and 38% by kaempferol (50 and 250 μM) and naringenin (50 and 250 μM), respectively (Fig. 2B).

Esterase Inhibition in Vitro and in Vivo in Rats. Hydrolysis of enalapril in rat liver microsomes or hydrolysis of lovastatin in rat liver S9 fraction was inhibited by both kaempferol and naringenin, two of the major flavonoids in GFJ. Kaempferol seemed to be a more potent esterase inhibitor than naringenin in the rat liver system. In vivo, the AUC of lovastatin acid was increased by 171, 246, 159, and 288% in rats following oral administration of lovastatin with kaempferol (2 and 10 mg/kg) and naringenin (2 and 10 mg/kg), respectively, compared with dosing with water (Table 2). Practically no unchanged lovastatin was detected in plasma, because of its rapid hydrolysis by plasma esterases. BNPP, a known esterase inhibitor, produced an effect similar to those of kaempferol and naringenin (Li et al., 2007). The positive BNPP effect suggested that the esterase plays a significant role in modulating the oral exposure to lovastatin. Thus, the large increase in AUC observed with kaempferol and naringenin was a combination of their effects due to CYP3A and esterase inhibition. To differentiate the modes of kaempferol and naringenin effects via CYP3A inhibition, esterase inhibition, and/or a combination of both, portal vein-cannulated rats were dosed with water or with kaempferol

TABLE 3

Portal plasma PK parameters of lovastatin, lovastatin acid, and 6′β-hydroxylovastatin following oral coadministration of lovastatin (10 mg/kg) with water and kaempferol (10 mg/kg)

Data are mean values ± standard deviation ($n = 4$).

Coadministration	Water			Kaempferol, 10 mg/kg		
	$AUC_{0-8\ h}$	T_{max}	C_{max}	$AUC_{0-8\ h}$	T_{max}	C_{max}
	nM · h	*h*	*nM*	*nM*	*h*	*nM*
Lovastatin	1440 ± 678	2.3 ± 0.7	358 ± 67	3662 ± 990*	2.4 ± 2.0	985 ± 410
Lovastatin acid	3960 ± 482	2.1 ± 2.5	1042 ± 191	8420 ± 2698*	2.5 ± 1.7	2425 ± 946
6′β-Hydroxylovastatin	93 ± 49	1.6 ± 0.9	60 ± 39	286 ± 143*	3.1 ± 2.0	105 ± 51

* Statistically significantly difference ($P < 0.05$).

(10 mg/kg). The portal plasma exposure of lovastatin acid, lovastatin, and 6′β-hydroxylovastatin with kaempferol showed 113, 154, and 208% higher AUC values than did dosing with water. Once absorbed, lovastatin is rapidly converted to lovastatin acid in rat plasma with a half-life shorter than 5 min. Lovastatin is known to be metabolized by CYP3A to 6′β-hydroxylovastatin as one of the major oxidized products (Halpin et al., 1993). The possible effect of kaempferol on lovastatin exposure by inhibiting intestinal CYP3A was examined by comparing the AUC ratio of oxidized metabolite 6′β-hydroxylovastatin to lovastatin. The 6′β-hydroxylovastatin was identified by LC/MS/MS spectral comparison with the published data (Halpin et al., 1993) and quantitated in plasma using lovastatin standard curves. The AUC ratio of 6′β-hydroxylovastatin to lovastatin stayed low at 0.064 and 0.078 for coadministration with water and kaempferol, respectively (Table 3), indicating that kaempferol did not markedly inhibit CYP3A activity in rats. This finding is consistent with findings in the literature that kaempferol and naringenin are weak CYP3A inhibitors with IC_{50} values greater than 100 μM (Ho et al., 2001). In general, the absorption of GFJ components is considered to be poor, and their action is postulated to be mainly in the small intestine (Schmiedlin-Ren et al., 1997; He et al., 1998).

The exposure to enalaprilat was also increased by 18, 38, 60, and 109% in rats following oral administration of enalapril with naringenin (2 and 10 mg/kg) and kaempferol (2 and 10 mg/kg), respectively, compared with dosing with water (Fig. 5; Table 2). Enalapril is only metabolized by carboxylesterase (hCE1), and is not a CYP3A substrate; thus, the esterase inhibition by kaempferol and naringenin led to an increase of enalaprilat after oral exposure in rats. This is consistent with the increased exposure of enalapril when coadministered with the esterase inhibitor BNPP (Li et al., 2007), as well as with the in vitro data.

Overall, the study identified the flavonoids as active components in grapefruit juice that are partly responsible for esterase-inhibitory activity in vitro in rat liver, in human liver and Caco-2 systems, and in vivo in rats. Two of the flavonoids, kaempferol and naringenin, showed significant exposure increases for the active acids in rats when coadministered with lovastatin and enalapril. The results show that the flavonoids have the potential of being used clinically to selectively inhibit esterase activity for enhancing the oral absorption of ester prodrugs.

Acknowledgments. We thank Kym Cardoza for excellent support with animal in-life studies, and Dr. Cindy Q. Xia and Ning Liu for invaluable guidance on transport studies.

References

Bailey DG, Arnold JM, Munoz C, and Spence JD (1993) Grapefruit juice-felodipine interaction: mechanism, predictability, and effect of naringin. *Clin Pharmacol Ther* 53:637–642.

Bailey DG, Kreeft JH, Munoz C, Freeman DJ, and Bend JR (1998) Grapefruit juice-felodipine interaction: effect of naringin and 6′,7′-dihydroxybergamottin in humans. *Clin Pharmacol Ther* 64:248–256.

Bailey DG, Spence JD, Edgar B, Bayliff CD, and Arnold JM (1989) Ethanol enhances the hemodynamic effects of felodipine. *Clin Invest Med* 12:357–362.

Bailey DG, Spence JD, Munoz C, and Arnold JM (1991) Interaction of citrus juices with felodipine and nifedipine. *Lancet* 337:268–269.

De Castro WV, Mertens-Talcott S, Rubner A, Butterweck V, and Derendorf H (2006) Variation of flavonoids and furanocoumarins in grapefruit juices: a potential source of variability in grapefruit juice-drug interaction studies. *J Agric Food Chem* 54:249–255.

Edwards DJ, Bellevue FH 3rd, and Woster PM (1996) Identification of 6′,7′-dihydroxybergamottin, a cytochrome P450 inhibitor, in grapefruit juice. *Drug Metab Dispos* 24:1287–1290.

Fukuda K, Ohta T, Oshima Y, Ohashi N, Yoshikawa M, and Yamazoe Y (1997) Specific CYP3A4 inhibitors in grapefruit juice: furocoumarin dimers as components of drug interaction. *Pharmacogenetics* 7:391–396.

Guo LQ, Fukuda K, Ohta T, and Yamazoe Y (2000) Role of furanocoumarin derivatives on grapefruit juice-mediated inhibition of human CYP3A4 activity. *Drug Metab Dispos* 28:766–771.

Halpin RA, Ulm EH, Till AE, Kari PH, Vyas KP, Hunninghake DB, and Duggan DE (1993) Biotransformation of lovastatin. V. Species differences in in vivo metabolite profiles of mouse, rat, dog, and human. *Drug Metab Dispos* 21:1003–1011.

He K, Iyer KR, Hayes RN, Sinz MW, Woolf TF, and Hollenberg PF (1998) Inactivation of cytochrome P450 3A4 by bergamottin, a component of grapefruit juice. *Chem Res Toxicol* 11:252–259.

Ho PC, Saville DJ, Coville PF, and Wanwimolruk S (2000) Content of CYP3A4 inhibitors, naringin, naringenin and bergapten in grapefruit and grapefruit juice products. *Pharm Acta Helv* 74:379–385.

Ho PC, Saville DJ, and Wanwimolruk S (2001) Inhibition of human CYP3A4 activity by grapefruit flavonoids, furanocoumarins and related compounds. *J Pharm Pharm Sci* 4:217–227.

Jignesh P, Balasubrahmanyam B, Surajit D, Mitra D, and Ashim K (2004) In vitro interaction of the HIV protease inhibitor Ritonavir with herbal constituents: changes in P-gp and CYP3A4 activity. *Am J Ther* 11:262–277.

Li P, Callery PS, Gan LS, and Balani SK (2007) Esterase inhibition attribute of grapefruit juice leading to a new drug interaction. *Drug Metab Dispos* 35:1023–1031.

Rashid J, McKinstry C, Renwick AG, Dirnhuber M, and George CF (1993) Quercetin, an in vitro inhibitor of CYP3A, does not contribute to the interaction between nifedipine and grapefruit juice. *Br J Clin Pharmacol* 36:460–463.

Ross SA, Ziska DS, Zhao K, and Elsohly MA (2000) Variance of common flavonoids by brand of grapefruit juice. *Fitoterapia* 71:154–161.

Schmiedlin-Ren P, Edwards DJ, Fitzsimmons ME, He K, Lown KS, Woster PM, Rahman A, Thummel KE, Fisher JM, Hollenberg PF, et al. (1997) Mechanisms of enhanced oral availability of CYP3A4 substrates by grapefruit constituents. Decreased enterocyte CYP3A4 concentration and mechanism-based inactivation by furanocoumarins. *Drug Metab Dispos* 25:1228–1233.

van Gelder J, Deferme S, Annaert P, Naesens L, De Clercq E, Van den Mooter G, Kinget R, and Augustijns P (2002) Intestinal absorption enhancement of the ester prodrug tenofovir disoproxil fumarate through modulation of the biochemical barrier by defined ester mixtures. *Drug Metab Dispos* 30:924–930.

Wadkins RM, Hyatt JL, Wei X, Yoon KJ, Wierdl M, Edwards CC, Morton CL, Obenauer JC, Damodaran K, Beroza P, et al. (2005) Identification and characterization of novel benzil (diphenylethane-1,2-dione) analogues as inhibitors of mammalian carboxylesterases. *J Med Chem* 48:2906–2915.

Wadkins RM, Hyatt JL, Yoon KJ, Morton CL, Lee RE, Damodaran K, Beroza P, Danks MK, and Potter PM (2004) Discovery of novel selective inhibitors of human intestinal carboxyl esterase for the amelioration of irinotecan-induced diarrhea: synthesis, quantitative structure-activity relationship analysis, and biological activity. *Mol Pharmacol* 65:1336–1343.

Xia CQ, Liu N, Yang D, Miwa G, and Gan L-S (2005) Expression, localization and functional characterization of breast cancer resistance protein in Caco-2 cells. *Drug Metab Dispos* 33:637–643.

Address correspondence to: Ping Li, Biogen Idec, Inc. 15 Cambridge Center, Cambridge, MA 02142. E-mail: ping.li@biogenidec.com

ACADEMIC PRESS

Pharmacological Research 48 (2003) 601–606

Pharmacological research

www.elsevier.com/locate/yphrs

Comparative study of flavonoids in experimental models of inflammation

Alejandra Ester Rotelli*, Teresita Guardia, Américo Osvaldo Juárez, Nadir Ernesto de la Rocha[1], Lilian Eugenia Pelzer

Cátedra de Farmacología, Facultad de Química, Bioquímica y Farmacia, Universidad Nacional de San Luis, Chacabuco y Pedernera, 5700 San Luis, Argentina

Accepted 30 June 2003

Abstract

The anti-inflammatory activities of flavonols (quercetin, rutin and morin) and flavanones (hesperetin and hesperidin) were investigated in animal models of acute and chronic inflammation. Rutin was only effective in the chronic process, principally in adjuvant arthritis. On neurogenic inflammation induced by xylene, only the flavanones were effective; besides, these compounds were the most effective on subchronic process. The most important compound in reducing paw oedema induced by carrageenan was quercetin.

Keywords: Flavonoids; Anti-inflammatory activity; Animal inflammation models; Adjuvant arthritis

1. Introduction

The inflammatory process involves a series of events that can be elicited by numerous stimuli, for example, infection agents, ischemia, antigen–antibody interactions, chemical, thermal or mechanical injury. The inflammatory responses occur in three distinct phases, each apparently mediated by different mechanisms: an acute one characterized by local vasodilatation and increased capillary permeability, a subacute phase characterized by infiltration of leukocyte and phagocyte cells and a chronic proliferative phase, in which tissue degeneration and fibrosis occur.

Many potential anti-inflammatory agents are evaluated in the pharmaceutical industry and animal models are used extensively in the testing of them. Winter et al. [1], showed in rats that acute inflammatory response to carrageenan is a local process and is not know to be antigenic. Acute inflammation generated by carrageenan induces the activation of gelatinases and collagenases [2]. Turner [3] and Di Rosa et al. [4] reported that the carrageenan induced inflammatory process in the rat involves three phases: an initial release of histamine and serotonin (first 1.5 h), a second phase mediated by kinins (1 h following phase 1) and last, a third phase mediated by prostaglandins. Therefore, seems to produce an inflammatory response by a mechanism different from that of agents such as xylene or the anaphylactic reaction towards dextran. Xylene induces a neurogenic inflammation when it is applied topically. This inflammation has begun to emphasize the cellular mechanisms involved in regulating the release of pro-inflammatory substances from sensory neurones [5]. The cotton wool granuloma described first by Meier et al. [6] reflects the chronic proliferative inflammation. On the other hand, adjuvant-induced arthritis (AIA) is developed after injection of complete Freund's adjuvant into rats [7]. It is a systemic disease with articular and visceral manifestation that resembles rheumatoid arthritis. It is characterized by chronic evolution with recurrent inflammatory bouts resulting in periarticular, articular and bone lesion [8]. Pearson described it originally in 1956 using Wistar rats [9]. Although the etiology of AIA is not well understood.

Flavonoids are compounds biosynthesized by most of plants and were found to possess significant activity on the inflammatory process [10]. Therefore, the current study was designed to investigate comparative efficacy of flavonols: rutin, quercetin and morin, and flavanones: hesperidin and hesperetin (Fig. 1), on different models of acute and subchronic inflammation and adjuvant arthritis.

* Corresponding author. Tel.: +54-2652-424689; fax: +54-2652-431301.
E-mail address: arotelli@unsl.edu.ar (A.E. Rotelli).
[1] Becario del Colegiode farmacéuticos de la Provincia de Buenos Aires, Argentina.

1043-6618/$ – see front matter © 2003 Elsevier Ltd. All rights reserved.
doi:10.1016/S1043-6618(03)00225-1

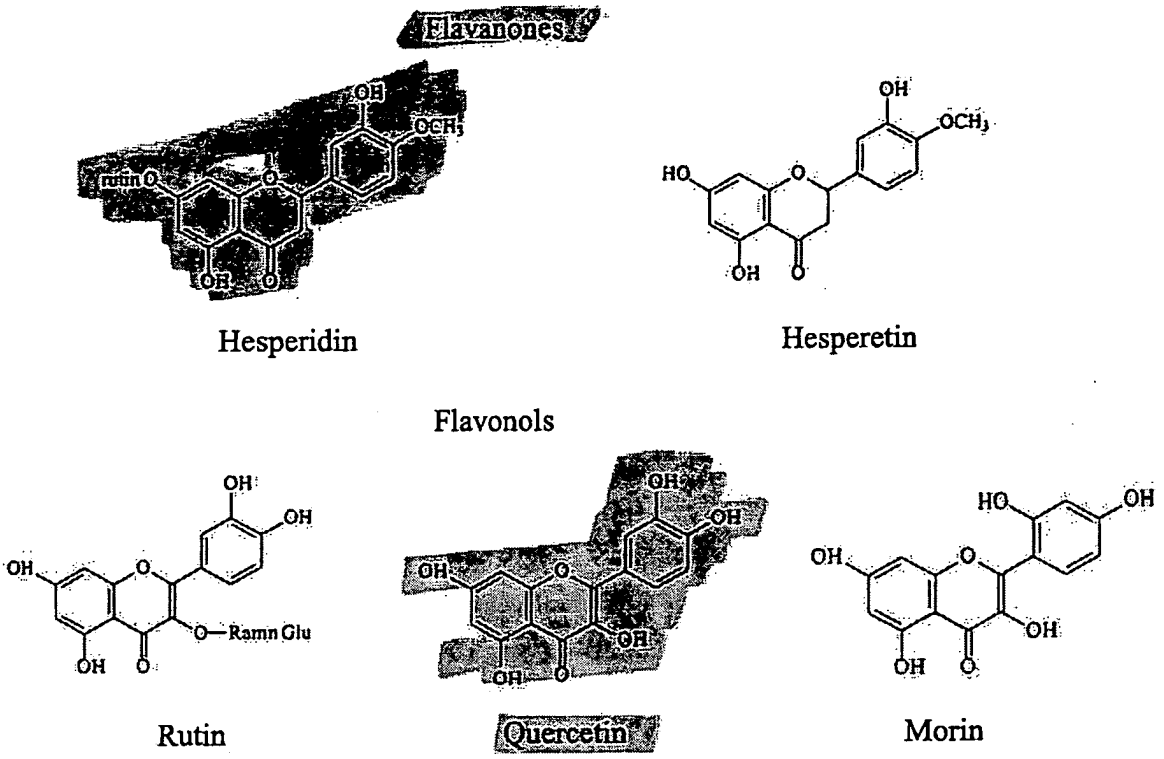

Fig. 1. Structures of compound tested.

2. Material and methods

2.1. Animals

Rockland mice weighing 30–35 g and Wistar albino rats weighing 160–180 g fed on standard chow and tap water ad libitum were used. The animals were housed at a room temperature of 24 ± 1 °C with 12 h light/dark cycle. The animals were randomly assigned to different group and a period of 4 days was allowed for adaptation on each experiment.

2.2. Drugs

Complete Freund's adjuvant, phenylbutazone and carrageenan type IV were purchased from Sigma, USA.

3. Experimental procedure

3.1. Methods for testing acute inflammation

3.1.1. Carrageenan-induced paw in mice

The mice were injected with carrageenan in the paw to produce acute inflammation. A total of 42 mice were divided into seven groups of six. Group 1 served as a control and received normal saline. Group 2 was administered with an intraperitoneal injection of phenylbutazone (80 mg kg^{-1}). Groups 3, 4, 5, 6 and 7 were injected intraperitoneally with rutin (150 mg kg^{-1}), hesperidin (150 mg kg^{-1}), quercetin, morin and hesperetin (75 mg kg^{-1}), respectively. All drugs were suspended in normal saline and were administered 1 h before the carrageenan 3.5% injection.

Paw volume was measured by the volume displacement technique using a plesthymometer Ugo Basile (Italy), it was sensitive to 0.01 ml volume changes, pre-treatment and post-treatment of carrageenan at 1, 3, 5 and 7 h. Percentage inhibition of inflammation induced by each was calculated with respect to its vehicle treated control group [11].

3.1.2. Xylene induced ear oedema

Mice were divided into seven groups of six each. One hour after intraperitoneal injection of the flavonoids (0.25 M kg^{-1}), 0.03 ml of xylene was applied to the anterior and posterior surfaces of the right ear. The left ear was considered as control. Thirty minutes after xylene application, mice were killed by euthanasia within an atmosphere of ether and both ears were removed. Circular sections were taken, using a cork borer with a diameter of 7 mm,

and weighed. The increase in weight caused by the irritant was measured by subtracting the weight of the untreated left ear section from that of the treated right ear section [12].

3.2. Method for testing the proliferative phase (granuloma formation)

3.2.1. Cotton pellet granuloma

A total of 35 rats were anaesthetized with ether. The back skin was shaved and disinfected with 70% ethanol. An incision was made in the lumbar region. Using a blunted forceps subcutaneous tunnels were formed and sterilized cotton pellet weighing 50 mg was introduced. The animals were divided into seven groups of six rats. Five groups were treated subcutaneously with rutin and hesperidin 50 mg kg^{-1} and quercetin, morin and hesperetin 25 mg kg^{-1} once daily for six consecutive days. In another group, dexamethasone 7 mg kg^{-1} was administered subcutaneously as a standard anti-inflammatory drug, whereas normal saline was injected to the control group. On day 7, the rats were killed by ether and the cotton pellets were excised and were dried until the weight remains constant. The increase in the pellet weight was considered as granuloma tissue deposit [6].

3.3. Method for experimental arthritis

3.3.1. Adjuvant arthritis

Experimental arthritis was induced in rats according to the method of adjuvant–carrageenan-induced inflammation (ACII) [13]. A total of 49 rats were divided into control, standard and test groups of seven animals each. On day 0, all of them received an injection of 0.1 ml Freund's complete adjuvant intradermally at the base of the tail. Six days after the adjuvant inoculation (day 6), a suspension of 0.1 ml of carrageenan (2%, w/v in saline solution) was injected in the subplantar region of the left hind paw of the rat, 1 h after intraperitoneal administration of the rutin, quercetin, hesperedin, morin, indomethacin and phenylbutazone. The degree of pedal oedema was determined by measuring both hind paws volume by plethysmograph (Ugo Basile). Plethysmographic measurements were made before the adjuvant injection (day 0), and were repeated again 6 days later at 3 and 5 h (acute phase) and discontinued from days 7 to 21 (chronic phase) after carrageenan injection.

Rutin, quercetin, hesperidin and morin (test groups) in doses of 75 mg kg^{-1}, phenylbutazone (80 mg kg^{-1}) and indomethacin (6 mg kg^{-1}) (standard group) were administered intraperitoneally 1 h before the carrageenan injection and once every day at the same time throughout the experiment. The vehicle used was saline solution. The inhibition percentage of oedema was calculated for each animal group in comparison with control group.

3.4. Statistical analysis

Data obtained from pharmacological experiment are expressed as mean values ± S.D. Differences between the control and the treatments in this experiment were tested for significance using analysis of variance followed by Dunnet's test. A probability of $P < 0.05$ was considered significant; a probability of $P < 0.01$ was considered very significant.

4. Results

4.1. Effect on carrageenan-induced paw in mice

The results of the treatment with test agent were shown in Table 1. As can be seen, quercetin, hesperetin and morin showed significant inhibition. Quercetin had the highest anti-inflammatory effect. Morin inhibited the inflammatory process at 3 and 5 h, while hesperetin did it only at 3 h. No significant activity was detected by glycoside flavonoids, rutin and hesperidin.

Table 1
Effect of intraperitoneal doses of flavonoids on carrageenan-induced paw oedema in mice

Treatment	Doses (mg kg^{-1})	1 h		3 h		5 h		7 h	
		Oedema volume (μl)	Inhibition (%)	Oedema volume (μl)	Inhibition (%)	Oedema volume (μl)	Inhibition (%)	Oedema volume (μl)	Inhibition (%)
Control		137 ± 40	–	182 ± 40	–	145 ± 40	–	182 ± 51	–
Rutin	150	139 ± 50	–	104 ± 31	43	150 ± 50	–	190 ± 56	–
Quercetin	75	47 ± 35	66*	82 ± 43	55**	72 ± 28	53**	68 ± 13	63**
Morin	75	136 ± 49	1	110 ± 34	46*	68 ± 31	55**	142 ± 36	22
Hesperidin	150	140 ± 55	–	120 ± 55	34	147 ± 46	–	188 ± 51	–
Hesperetin	75	89 ± 54	35	94 ± 29	48**	121 ± 52	16	129 ± 16	29*
Phenylbutazone	80	109 ± 42	20	128 ± 23	39**	72 ± 28	50**	91 ± 45	50*

The increase in volume caused by carrageenan was measured by subtracting the volume of the untreated right paw from that of the treated left paw. Inhibition (%) represent percentage reduction paw volume compared with the controls. Values are the mean ± S.D. for six mice.

* $P < 0.05$ (Dunnet's test).

** $P < 0.01$ (Dunnet's test).

Table 2
Effect of the intraperitoneal doses of flavonoids on xylene-induced ear swelling in mice

Treatment	Dose ($M\,kg^{-1}$)	Ear swelling (mg)	Inhibition (%)
Control		30.1 ± 5.6	–
Rutin	0.25	27.3 ± 7	9
Quercetin	0.25	26.5 ± 8.9	12
Morin	0.25	22.1 ± 3.1	26
Hesperidin	0.25	16.6 ± 9.2	45**
Hesperetin	0.25	16.9 ± 5.9	44**

The increase in weight caused by the irritant (xylene) was measured by subtracting the weight of the untreated left ear section from that of the treated right ear sections. Inhibition (%) represent percentage reduction ear weight compared with the controls. Values are the mean ± S.D. for six mice.

** $P < 0.01$, compared to control (normal saline) (Dunnet's test).

4.2. Effect on xylene induced ear oedema

The results present in Table 2 showed that only the flavanone hesperidin and hesperetin exerted a significant anti-inflammatory effect in this model.

4.3. Effect on cotton pellet granuloma

In the anti-inflammatory study using cotton pellet (Table 3), the five compounds produced significantly reduce in the granuloma formation, but morin followed by hesperidin and hesperetin exerted the more significant protective effects.

4.4. Effect on adjuvant arthritis

The effect of flavonols (rutin, quercetin and morin) and flavanone (hesperidin) were shown in Table 4.

Rutin, quercetin and morin decreased the oedema produced in the acute phase, induced 3–5 h after carrageenan (day 6) but hesperidin was active only at 3 h.

In the chronic phase (7–21 days) only rutin was significantly active all the days. Quercetin had no significant action on the 7, 12 and 21 days, while morin showed no significant action on 8 and 20 days during the chronic phase. Hesperidin showed no significant activity on days 9, 14, 19 and 16.

Table 3
Effect of the subcutaneous doses of flavonoids on cotton pellet granuloma test

Treatment	Doses ($mg\,kg^{-1}$)	Granuloma weight (mg)	Inhibition (%)
Control	–	855 ± 73	–
Rutin	50	650 ± 45	24*
Quercetin	25	633 ± 65	26*
Morin	25	487 ± 87	43**
Hesperidin	50	598 ± 63	30**
Hesperetin	25	616 ± 43	28**
Dexamethasone	7	427 ± 36	50***

Inhibition (%) represent percentage reduction of granuloma weight compared with the controls. Values are the mean ± S.D. for six rats.

* $P < 0.01$ (Dunnet's test).

** $P < 0.005$ (Dunnet's test).

*** $P < 0.001$ (Dunnet's test).

5. Discussion

Flavonoids are polyphenolic compounds that occur ubiquitously in foods of plant origin. Variations in the heterocyclic ring C give rise to flavonols, flavones, catechins, flavanones, anthocyanidins and isoflavonoids [14]. Biological assays using isolated compounds reveal that flavonoids exhibit a wide range of effects on biological systems. They have been shown to exert antimicrobial, antiviral, antiulcerogenic, antineoplasic, antihepatotoxic, hypolipidemic, antiallergic and anti-inflammatory activities [15]. Biochemical investigations of the flavonoid mechanisms of action have shown that these compounds inhibit a wide variety of enzymatic systems. The ability of certain flavonoids to inhibit both cyclooxygense and 5-lipooxygenase pathways of the arachidonate metabolism may contribute to the anti-inflammatory properties [16]. On the other hand, flavonoids are known to display many antioxidant properties including scavenging free radicals and preventing lipid peroxidation [17]. These activities seem to be directly related to the number of hydroxyl group at ring B [18]. In the present study, flavonols and flavanones exhibit sizable anti-inflammatory effects.

Quercetin, morin (flavonols) and hesperetin (flavanone) produced an anti-inflammatory effect on the acute inflammatory process like that induced by carrageenan, which was higher than observed after phenylbutazone administration. Rutin and hesperedin did not show any significant activity. According to Di Rosa et al. [4] and Vinegér et al. [19,20], histamine and serotonin were mainly released during first 1.5 h after carrageenan injection. Kinin was released from 1.5 to 2.5 h and at the last step inflammation was continued until 5 h by prostaglandins. From the results obtained in this work, the intraperitoneal administration of quercetin produced significant inhibition along the experiment, while morin and hesperidin effect might correlate with the release of kinin.

In the cellular mechanism of neurogenic inflammation induced by xylene [5], there are a number of potential substances released from capsaicin-sensitive sensory neurones, most evidence supports the notion that the neuropeptides, substance P, are major initiators of inflammation. It was very interesting to observe that only flavanones hesperidin and hesperetin were involved in these inflammatory process.

Comparisons were made between flavanones and flavonols in the proliferative phases of inflammation. Our findings demonstrate that both are capable of inhibiting the development of cotton pellet induced granuloma.

Inflammation in rheumatoid arthritis involves complex response of chemical mediators, chemotactic factors, leukocytes and phagocytes causing injury to cartilage and other tissues. Beneficial effect of flavonoids was demonstrated.

Table 4
Effects of intraperitoneal treatment of flavonoids, indomethacin and phenylbutazone on adjuvant–carrageenan-induced

Time	Control	Rutin		Quercetin		Hesperedin		Morin		Phenylbutazone		Indomethacin	
	Paw volume	Paw volume	Inhibition (%)	Paw volume	Reduction (%)	Paw volume	Reduction (%)	Paw volume	Reduction (%)	Paw volume	Reduction (%)	Paw volume	Reduction (%)
3 h (6 days)	132 ± 35	63 ± 19	53**	55 ± 20	59**	63 ± 10	52**	65 ± 12	49**	73 ± 12	45*	66 ± 25	50**
5 h (6 days)	114 ± 29	60 ± 2	47**	71 ± 19	37*	94 ± 25	35*	70 ± 9	38**	76 ± 16	33*	68 ± 23	40**
7 days	102 ± 15	52 ± 19	48**	82 ± 29	20	65 ± 8	36*	67 ± 10	35*	72 ± 16	29	63 ± 18	38*
8 days	94 ± 17	60 ± 13	36**	57 ± 7	39**	53 ± 26	44*	75 ± 12	20	68 ± 11	27*	59 ± 15	37*
9 days	95 ± 24	36 ± 16	61**	41 ± 10	57**	69 ± 15	27	66 ± 6	30*	59 ± 12	38*	48 ± 11	51**
10 days	90 ± 27	35 ± 8	61**	27 ± 8	70**	48 ± 9	47**	61 ± 6	32*	44 ± 7	54**	53 ± 9	41*
12 days	62 ± 12	29 ± 17	53*	37 ± 13	40*	38 ± 18	38*	42 ± 10	33*	50 ± 12	19	51 ± 12	18
14 days	74 ± 19	33 ± 19	55**	31 ± 8	58**	47 ± 10	36*	32 ± 15	57**	67 ± 14	9.5	70 ± 12	5
16 days	93 ± 25	49 ± 16	47*	34 ± 18	63**	64 ± 2	31*	55 ± 19	41*	60 ± 18	35	72 ± 15	22
19 days	136 ± 36	84 ± 17	38*	71 ± 19	47**	138 ± 19	–	101 ± 12	26	96 ± 18	29	131 ± 23	4
21 days	100 ± 30	59 ± 22	41*	59 ± 13	41*	71 ± 10	29*	52 ± 15	48*	88 ± 20	12	83 ± 15	17

Increase in paw volume (μl) (mean ± S.D.) (inhibition (%)). Tabular values represent the mean ± S.D. of increase in paw volume for seven rats. Values indicate percentage reduction in paw volume compared with the controls.

* $P < 0.05$ (significance relative to control values).

** $P < 0.01$ (significance relative to control values).

However, rutin had the highest effect in the experimental arthritis.

In conclusion, the present study shows marked anti-inflammatory action by tested agents in different inflammation models and we could infer that rutin was only effective in the chronic process like arthritis. The flavanones hesperidin and hesperetin were the only effective compounds on neurogenic inflammation induced by xylene and they were the most effective on subchronic process. Moreover, the most important compound in reduce the paw oedema induced by carrageenan was quercetin.

Acknowledgements

The authors are grateful to the Department of Organic Chemistry, University of San Luis, for providing the plant flavonoids.

References

[1] Winter C, Risley E, Nuss G. Carrageenan-induced edema in hind paw of rats as an assay for anti-inflammatory drug. Proc Soc Exp Biol Med 1962;111:207–10.
[2] Nakagawa H, Sakata K. Partial purification and characterization of exudate gelatinase in the acute phase of carrageenan-induced inflammation in rats. J Biochem 1996;100:1499–506.
[3] Turner RA. Screening methods in pharmacology, vol. 1. New York: Academic Press; 1965. p. 100–58.
[4] Di Rosa M, Giround JP, Willougbby DA. Studies of the mediators of the acute inflammatory response induced in rats in different sites by carrageenan and turpentine. J Pathol 1971;104:15–29.
[5] Richardson JD, Vasko MR. Cellular mechanisms of neurogenic inflammation. J Pharmacol Exp Ther 2002;302(3):839–45.
[6] Meier R, Schuler W, Desaulles P. Zur Frage des Mechanismus der Hemmung des Bindegewebswachstums durch. Cortisone Experientia 1950;VI/12(12):469–71.
[7] Billingham MEJ. Models of arthritis and the search for antirrheumatic drugs. Pharmacol Ther 1983;21:399.
[8] Pearson CM, Wood FD. Studies of polyarthritis and other lesions induced in rats, by injection of mycobacterial adjuvant. I. General clinical and pathologic characteristics and some modifying factors. Arthritis Rheum 1959;2:440.
[9] Pearson CM. Development of arthritis, periarthritis and periostitis in rats given adjuvants. Proc Soc Exp Biol Med 1956;91:95.
[10] Handa SS, Chawla AS, Sharma AK. Plants with anti-inflammatory activity. Fitoterapia LXIII 1992;3:31.
[11] Sugishita E, Amagaya S, Ogihara Y. Anti-inflammatory testing methods: comparative evaluation of mice and rats. J Pharm Dyn 1981;4:565–75.
[12] Young JM, De Young LM. Cutaneous models of inflammation for the evaluation of topical and systemic pharmacological agents. In: Spector J, Back N, editors. Pharmacological methods in the control of inflammation, New York: Liss; 1989. p. 215–31.
[13] Mizushima Y, Tsukada M, Akimoto T. A modification of rat adjuvant arthritis for testing arthritis for testing antirrheumatic drugs. J Pharm Pharmacol 1972;24:781–5.
[14] Hollman PCH, Katan MB. Absorption, metabolism and health effect of dietary flavonoids in man. Biomed Pharmacother 1997;51:305–10.
[15] Di Carlo G, Mascolo N, Izzo AA, Capasso F. Flavonoids: old and new aspects of a class of natural therapeutic drugs. Life Sci 1999;65:337–53.
[16] Williams CN, Honet JRS, Harbone JB, Greenham J, Eeagles J. A biologically active lipophilic flavonols from *Tanacetum parthenium*. Phytochemistry 1995;38:267–70.
[17] Torel J, Cillard J, Cillard P. Antioxidant activity of flavonoids and reactivity with peroxyradical. Phytochemistry 1986;25:383–5.
[18] Husaim SR, Cillard J, Cillard P. Hydroxyradical scavenging activity of flavonoids. Phytochemistry 1987;26:2489–91.
[19] Vineger R, Truax JF, Selph JL. Quantitative studies of the pathway to acute carrageenan inflammation. Fed Proc 1976;35:2447–56.
[20] Vineger R, Truax JF, Selph JL, Vowelker FA. Pathway of onset development and decay of carrageenan pleuresy in the rat. Fed Proc 1982;41:2588–95.

668 J. Agric. Food Chem. 2010, 58, 668–675
DOI:10.1021/jf902680n

JOURNAL OF AGRICULTURAL AND FOOD CHEMISTRY
ARTICLE

Molecular Mechanism of Hesperetin-7-*O*-glucuronide, the Main Circulating Metabolite of Hesperidin, Involved in Osteoblast Differentiation

ANNA TRZECIAKIEWICZ,[†] VERONIQUE HABAUZIT,[†] SYLVIE MERCIER,[†] DENIS BARRON,[†] MIREIA URPI-SARDA,[†,§] CLAUDINE MANACH,[†] ELIZABETH OFFORD,[‡] AND MARIE-NOELLE HORCAJADA*[,†,‡,∥]

[†]INRA Clermont-Ferrand/Theix. Human Nutrition Unit UMR1019, F-63122 St. Genes Champanelle, France, [‡]Nestle Research Center, Vers-Chez-Les-Blanc, 1000 Lausanne 26, Switzerland, and [§]University of Barcelona, XaRTA, INSA. Pharmacy Faculty. Nutrition and Food Science Department, E-08028 barcelona, Spain. [∥]Current address: Department of Nutrition & Health, Nestlé Research Center, P.O. Box 44. CH-1000 Lausanne 26, Switzerland.

Citrus fruit hesperidin is hydrolyzed by gut microflora into aglycone form (hesperetin) and then conjugated mainly into glucuronides. We previously demonstrated that hesperetin enhanced osteoblast differentiation. In this study, we examined the effect of hesperetin-7-*O*-glucuronide (Hp7G) on primary rat osteoblast proliferation and differentiation. The impact of Hp7G on specific bone signaling pathways was explored. Osteoblasts were exposed to physiological concentrations of 1 (Hp7G1) and 10 (Hp7G10) μM of conjugate. The glucuronide did not affect proliferation but enhanced differentiation by significantly increasing alkaline phosphatase (ALP) activity from day 14 of exposure. Hp7G significantly induced mRNA expression of ALP, Runx2, and Osterix after 48 h of exposure. Moreover, phosphorylation of Smad1/5/8 was enhanced by Hp7G, while ERK1/2 remained unchanged after 48 h. Hp7G decreased RANKL gene expression. These results suggest that Hp7G may regulate osteoblast differentiation through Runx2 and Osterix stimulation, and might be implicated in the regulation of osteoblast/osteoclast communication.

KEYWORDS: Flavonoid metabolite; hesperetin 7-*O*-glucuronide; osteoblast differentiation; Osterix; Runx2

INTRODUCTION

Hesperidin (hesperetin-7-*O*-rutinoside) is a glycoside flavonoid belonging to the flavanone subgroup, found mainly in citrus fruits. When absorbed, hesperidin is hydrolyzed by gut microflora into the aglycone form (hesperetin) and then conjugated by the phase II drug-metabolizing enzymes into glucuronides (87% of total metabolites of hesperetin), sulfates, or sulfoglucuronides (*1*, *2*). In rodents fed 0.5% hesperidin in the diet, the circulating concentrations of aglycone hesperetin ranged from 3.5 to 5.5 μM (*3*, *4*), while 1 μM was measured in humans (*1*). Several biological activities such as antioxidant, anti-inflammatory, analgesic, and lipid lowering effects (*5*) have been attributed to hesperidin and its metabolites. Some authors have shown that hesperidin inhibits bone loss in ovariectomized mice (*3*) or rats (*4*) and prevents bone loss in male orchidectomized rats (*6*). The mechanisms by which hesperidin may affect skeletal metabolism still remain unclear. Nevertheless, it was recently shown that hesperetin may regulate primary rat osteoblast differentiation through bone morphogenetic protein (BMP) signaling (*7*).

The metabolism of flavonoids is similar to that of xenobiotics (*8*). Even if conjugates have been presented as forms of elimination and detoxification, in vitro biological properties of flavonoid conjugates found in vivo were reported (*9*). One reported study tested conjugated forms in osteoblastic cells and demonstrated that quercetin-3-glucuronide was able to increase the bone sialoprotein mRNA level in osteoblast-like ROS 17/2.8 cells (*10*). Only two in vitro studies were performed using hesperetin conjugates such as glucuronides in skin fibroblast cells (*11*) and hesperetin 7-*O*-glucuronide and 5-nitro-hesperetin in cortical neurons (*12*). To date, no effect of hesperetin conjugate on osteoblasts has been reported.

The available studies reporting flavonoid effect on osteoblastic cells have been performed with aglycone compounds. These compounds were able to stimulate ALP activity, which is one of the major osteoblast differentiation markers probably by upregulation of expression of two transcription factors such as Runx2 and Osterix (*13*) strongly implicated in the regulation of osteoblast functions (*14*). Moreover, Runx2 has a central function in coordinating multiple signals including AP-1 (commonly composed of c-Jun/c-fos) and Smad factors, which are involved in osteoblast differentiation (*15*). Runx2 and Osterix also play a role in the BMP pathway that may, in turn, activate different signaling cascades and Smad-dependent and independent pathways, including ERK, JNK, and p38 MAPK (*16*). Within flavonoids, there is also evidence that they are susceptible to the influence of

*Corresponding author. Phone: +41 21 785 8130. Fax: +41 21 785 8925. E-mail: marienoelle.horcajada@rdls.nestle.com.

 Published on Web 11/18/2009

the OPG/RANKL/RANK regulatory triad implicated in the osteoblast and osteoclast relationship (*17*, *18*). Osteoblasts produce both receptor activator of nuclear factor-kappaB (RANK) ligand (RANKL) and osteoprotegerin (OPG). OPG acts as a decoy receptor for RANKL and thereby neutralizes its function in osteoclastogenesis. Bone homeostasis depends on the local RANKL/OPG ratio (*19*).

The aim of this study was to assess the effect of hesperetin conjugate on osteoblast functions and the molecular mechanisms involved. Thus, the influence of hesperetin-7-*O*-glucuronide (Hp7G) at physiologically relevant concentration (1 and 10 μM) was tested in primary rat osteoblasts.

MATERIALS AND METHODS

Synthesis of Hesperetin-7-*O*-glucuronide. Hesperetin 7-*O*-glucuronide (Hp7G) has been chemically prepared by glucuronidation of its suitable precursor using 2,3,4-triacetyl-D-methyl glucurono-pyranosyl-(*N*-phenyl)-2,2,2-trifluoroacetimidate, followed by acetate deprotection using zinc acetate, and methyl ester hydrolysis using Pig Liver Esterase, according to Boumendjel et al. (*20*). The purity of the synthesized molecule examined by HPLC was 100%.

Cell Culture. Primary osteoblasts were isolated from the calvaria of newborn Wistar rats (INRA, Theix, France) by enzymatic digestion as described previously (*21*). Cells were maintained in α-minimal essential medium (α-MEM) (GIBCO, Paisley, UK) with 10% heat-inactivated fetal bovine serum (FBS) and 1% penicillin/streptomycin (GIBCO, Paisley, UK) in 5% CO_2 at 37 °C conditions. Cells were seeded on type I collagen-coated (BD Biosciences, Bedford, USA) 96-well plates at a density of 3500 cells/w, in 60 mm Petri dishes (4×10^5 cells/dish) or in 100 mm Petri dishes (5×10^5 cells/dish), and cultured for 2 days in α-MEM to reach confluence (which correspond to day 0 of cell culture for treatment exposure duration). Cells were then exposed to different conditions: minimal medium (C−), minimal medium containing 50 μg/mL ascorbic acid, 5 mM β-glycerophosphate (C+, optimized medium), and minimal medium supplemented with 1 μM (Hp7G1) or 10 μM (Hp7G10) hesperetin-7-*O*-glucuronide (Hp7G). Hp7G was dissolved in DMSO. In every condition, the final concentration of DMSO in medium was 0.1%. The medium was changed every 2 days. All cell experiments were performed in triplicate.

Cellular Uptake. Eight percent confluent cells were exposed for 24 h to 40 μM hesperetin (Hp), hesperetin-7-*O*-glucuronide (Hp7G), or vehicle (0.1% DMSO). Culture medium was collected after 0, 8, and 24 h of exposition in the presence or absence of cells and extracted with 2.5 volumes MeOH/H_2O (70:30) acidified with 200 mM HCl. After centrifugation (14000 rpm for 4 min), extracts were analyzed by liquid chromatography−tandem mass spectrometry (HPLC-MS/MS). The recovery rate for the extraction of Hp7G and Hp from the culture medium was 86 and 75%, respectively.

After 24 h of exposure, cells were rinsed three times using PBS (Sigma, Steinheim, Germany) then exposed to 0.5 mL of MeOH/H_2O (70:30) acidified with 200 mM HCl and scraped using a cell scraper (BD Falcon, Bedford, USA). These extraction conditions, in particular the small volume of solvent added, were chosen to maximize the concentration of metabolites in the extracts in order to facilitate a qualitative analysis of the metabolite uptake; however, they were not optimized for the quantitative analysis of flavanones in the intracellular medium.

HPLC-MS/MS Analysis. Liquid chromatography (LC) analyses were performed using a Hewlett-Packard 1100 HPLC system (Agilent Technologies, Waldbronn, Germany) equipped with a quaternary pump and an autosampler. An Applied Biosystems API 2000 triple quadrupole mass spectrometer (PE Sciex, Ontario, Canada), equipped with a Turbo IonSpray source ionizing in the negative mode at 550 °C was used. Optimized parameters for the detection of Hp and Hp7G were the following: capillary voltage, −4500 V; collision gas, 5 (arbitrary units); and curtain gas, 30 (arbitrary units). Declustering potential, focusing potential, entrance potential, and collision energy were optimized with infusion experiments of Hp (−50 V, −350 V, −5 V, and −30 V, respectively) and Hp7G (−16 V, −350 V, −10 V, and −26 V, respectively).

A SymmetryShield RP18 column (Waters, Milford, MA, USA), 2.1 × 150 mm i.d., 5 μm, was used for chromatographic separation. Linear gradient elution was performed as follows: 0−20 min 85% A to 100% B, with 0.1% formic acid as mobile phase A and 100% acetonitrile as mobile phase B. The column was re-equilibrated for 10 min. The flow rate was 400 μL/min, and the injection volume was 20 μL.

Data were acquired using the multiple reaction monitoring (MRM) mode, monitoring the Hp transition (301/164) and the Hp7G transition (477/301).

Cell Proliferation. Cell proliferation was measured by determining DNA content on days 0, 5, 9, 14, and 19. Cells were incubated with 2 μg/mL of bisbenzimide H 33342 (Hoechst) in PBS at 37 °C. The total amount of DNA was measured with FLX800 Microplate Fluorescence Reader (Bio-Tek Instruments, Winooski, VT, USA) at 360 nm wavelength (excitation) and 460 nm (emission). Fold increase in cell number was calculated relative to the initial cell number on day 0 (value = 1).

ALP Activity Measurement. Enzymatic activity of alkaline phosphatase (ALP) was measured kinetically on treatment days 0, 5, 9, 14, and 19 according to the method described by Sabokbar et al. (*22*). Osteoblasts were lysed by the freeze−thaw cycle and homogenization into 200 μL of diethanoamine/magnesium chloride hexahydrate buffer at pH 9.8 (Sigma, Steinheim, Germany). Cell lysate (10 μL) was added to 200 μL of *p*-nitrophenyl phosphate solution (Sigma, Steinheim, Germany). Absorbance was measured at 405 nm, 30 °C, and every 2 min 30 s during 30 min using an ELX808 microplate reader (Bio-Tek Instruments, Winooski, VT, USA). ALP activity was expressed as μmol *p*-nitrophenol/hour/mg protein. Protein measurement was performed according to Bradford's method using the BioRad protein assay (BioRad, Munich, Germany).

Real-Time PCR. Upon confluence, cells were exposed to different media: C−, C+, Hp7G1, or Hp7G10 for 24 and 48 h. After 24 and 48 h of treatment, total RNA and proteins were isolated using the NucleoSpin RNA/Protein Kit (Macherey-Nagel, Hoerdt, France). Total RNA concentration and purity were measured with a NanoDrop spectrophotometer (Wilmington, USA). RNA integrity was checked using the RNA 6000 Nano Assay kit with an Agilent 2100 bioanalyzer (Agilent Technologies, Santa Clara, USA). Reverse transcription of RNA was performed using the Ready-To-Go, You-Prime First-Strand Beads Kit (Amersham Biosciences, Piscataway, USA). The SYBR Premix Ex Taq (Perfect Real Time) (TaKaRa, Shiga, Japan) was used to quantify gene expression by Real-Time PCR. The PCR (program, 95 °C-30 s; 40 cycles, 95 °C-5 s; 60 °C-35 s) was performed using Mastercycler Ep Realplex (Eppendorf, Hamburg, Germany). Target gene expression was normalized to the housekeeping gene β-actin. The $2^{-\Delta\Delta Ct}$ method was applied to calculate relative gene expression compared to the C− condition, which corresponds to a value of 1 (*23*). The primers used for PCR are listed in Table 1.

Western Blot Analysis. Upon confluence, cells were exposed to different media: C−, C+, Hp7G1, or Hp7G10 for 24 and 48 h. The concentration of proteins isolated using the NucleoSpin RNA/Protein kit (Macherey-Nagel, Hoerdt, France) was measured by a BC assay kit (Uptima Interchim, Montluçon, France). Twenty-five micrograms of total protein was subjected to a 10% SDS−polyacrylamide gel and transferred to Immobilon-P-PVDF membranes at 100 V for 1 h and 45 min. The membranes were blocked in 5% nonfat dry milk in TBS-T (0.5% Tween 20) buffer for 2 h. Blots were incubated with antiphospho-Smad1/5/8 or antiphospho-ERK1/2 (Cell Signaling, Beverly MA, USA) at a 1:1000 dilution for 1 h at room temperature, then probed with 1:2000 diluted antirabbit horseradish peroxidase (HRP) conjugated secondary antibody (Santa Cruz Biotechnology, Santa Cruz, USA) for 1 h at room temperature. The blot signals were detected by enhanced chemiluminescence (ECL Plus, Amersham GE Healthcare, Buckinghamshire, UK). After stripping in a buffer containing 0.7% β-mercaptoethanol, membranes were labeled with 1:500 diluted anti-Smad1/5/8 (Santa Cruz Biotechnology, Santa Cruz, CA, USA) or 1:1000 diluted anti-ERK1/2 (Cell Signaling, Beverly MA, USA) and probed with 1:5000 diluted secondary antibody.

Statistical Analysis. Results are expressed as mean ± SEM. ALP activity and cell proliferation on each day were analyzed using parametric one-way ANOVA, followed by multiple comparisons Fisher/LSD performed in XLSTAT version 7.5.2 (AddinSoft, Paris, France).

Nonparametric test−Wilcoxon signed rank test (compared to control C−; hypothetical median = 1) on GraphPad InStat 3 software (San Diego, CA, USA) was used for statistical analysis of gene expression. p-value < 0.05 was considered statistically significant.

RESULTS

An optimized medium (C+) was used as a positive control of differentiation, and Hp7G was added to minimal medium (C−) to observe its proper action and not in synergy with ascorbic acid.

Cellular Uptake. The cellular uptake of Hp and Hp7G in primary rat osteoblasts was determined by HPLC-MS/MS analysis after 24 h of cell exposure to 40 μM Hp or Hp7G.

The compound stability in the growth medium was followed over 24 h in the presence and absence of cells. No degradation of the aglycone was observed in the absence of cells. In the presence of cells exposed to the aglycone, a peak with the characteristic MS/MS transition of hesperetin−glucuronide (MRM 477/301) was detected in the medium after 8 and 24 h, in concentration increasing with time (**Figure 1**). This peak showed the same retention time (8.19 min) as the standard Hp7G, suggesting that this specific metabolite was produced by the cells exposed to the aglycone. A minor peak also appeared at the same MS/MS transition and slightly higher retention time (8.3 min), and may correspond to the hesperetin-4′-*O*-glucuronide. Glucuronidation must have occurred inside the cells since glucuronidases are not present at the surface of cell membranes.

When cells were exposed for 24 h to hesperetin, Hp but not Hp7G was detected in the cell extract (**Figure 2B**). The intracellular concentration of Hp7G was below the limit of detection (18.5 nmol/L) probably because Hp7G was exported outside the cells by transporters.

When cells were exposed to Hp7G, a small hydrolysis into Hp (0.15%) was observed in the medium after 8 h and slightly increased at 24 h (0.6%) (chromatograms not shown). A small hydrolysis of Hp7G was also observed in the medium after 24 h in

Table 1. Primer Sequences for Real-Time PCR

transcript	primers (5′-3′)	product size
β-actin	forward: AGTGTGACGTTGACATCCGTA	112 bp
	reverse: GCCAGAGCAGTAATCTCCTTCT	
Runx2	forward: CGATCTGAGATTTGTAGGCCG	159 bp
	reverse: TCATCAAGCTTCTGTCTGTGCC	
Osterix	forward: AAGAGGTTCACCCGCTCTGA	122 bp
	reverse: TGATGTTTGCTCAAGTGGTCG	
OPG	forward: GGGCGTTACCTGGAGATCG	125 bp
	reverse: GAGAAGAACCCATCTGGACATTT	
RANKL	forward: GGCCACAGCGCTTCTCAG	143 bp
	reverse: AGTGACTTTATGGGAACCCGAT	
Noggin	forward: CACTATCTACACATCCGCCCAG	110 bp
	reverse: AGCGTCTCGTTCAGATCCTTCT	
BMP2	forward: GCCAGGTGTCTCCAAGAGACAT	179 bp
	reverse: AGCTGGACTTAAGACGCTTCCG	
BMP4	forward: GACTTCGAGGCGACACTTCT	100 bp
	reverse: GCCGGTAAAGATCCCTCATGTA	
Smad1	forward: CCACAACCCTATTTCGTCGGT	102 bp
	reverse: ATCCTGTCTGACTTCTCCGTCC	
Smad5	forward: TGAACTGAACAACCGTGTCGG	151 bp
	reverse: CCTGGTGTTCTCGATGGTTGAG	
c-Jun	forward: CCTCCCGTCTGGTTGTAGGAAT	145 bp
	reverse: CCCTTGCAACACCCTCTTCTTC	
c-fos	forward: TTCACCCTGCCTCTTCTCAATGAC	82 bp
	reverse: GCCTTCAGCTCCATGTTGCTAATG	
ALP	forward: ACAGCCATCCTGTATGGCAA	97 bp
	reverse: GCCTGGTAGTTGTTGTGAGCA	
OPN	forward: AGCAAGAAACTCTTCCAAGCAA	129 bp
	reverse: GTGAGATTCGTCAGATTCATCCG	
OCN	forward: TATGGCACCACCGTTTAGGG	123 bp
	reverse: CTGTGCCGTCCATACTTTCG	

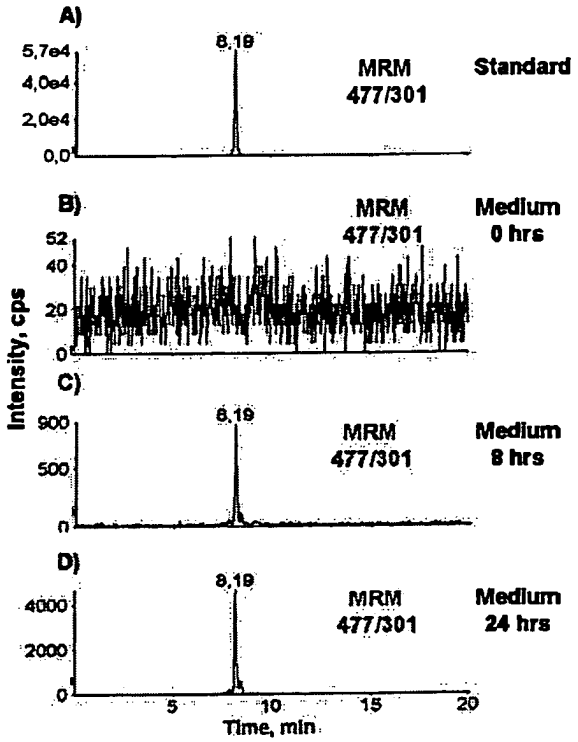

Figure 1. MRM trace chromatograms at hesperetin 7-*O*-glucuronide transition (477/301). (**A**) standard of hesperetin-7-*O*-glucuronide; (**B**) medium after 0 h of cell exposure to hesperetin; (**C**) medium after 8 h of cell exposure to hesperetin; (**D**) medium after 24 h of cell exposure to hesperetin.

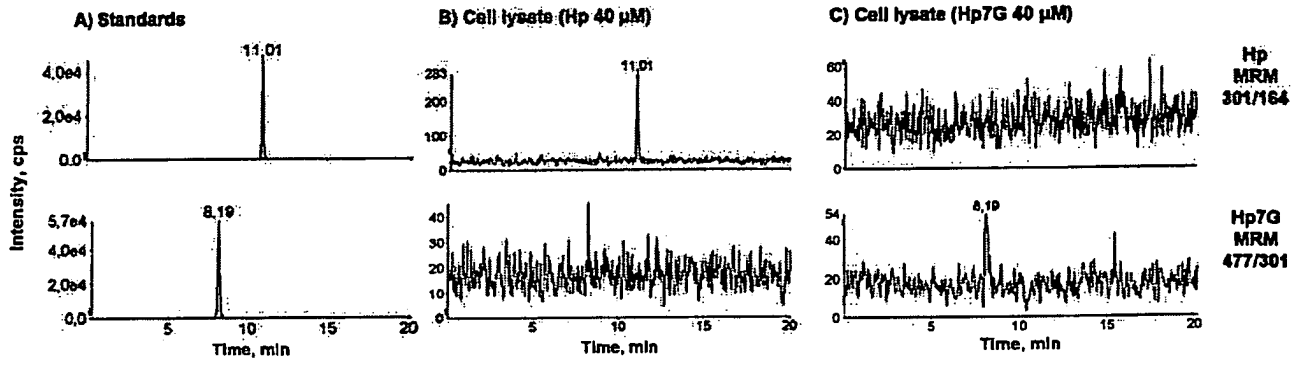

Figure 2. MRM trace chromatograms at hesperetin (301/164) and hesperetin-7-*O*-glucuronide (477/301) transitions from (**A**) standards; (**B**) cell lysate after 24 h of exposure to 40 μM Hp; and (**C**) cell lysate after 24 h of exposure to 40 μM Hp7G.

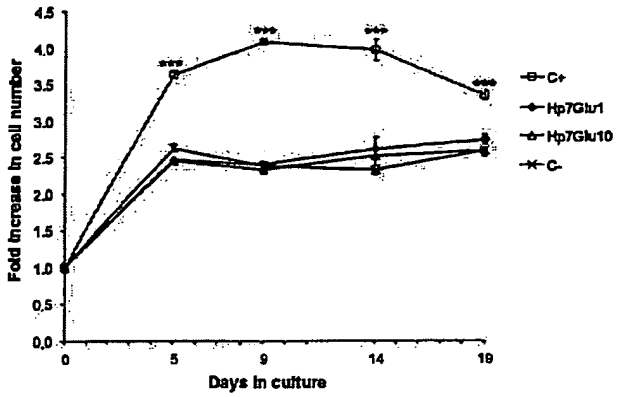

Figure 3. Proliferation of primary osteoblasts cultured in minimal medium (C−; ×), supplemented with 1 μM (Hp7G1; ◇) or 10 μM (Hp7G10; △) hesperetin 7-*O*-glucuronide, or in optimized medium (C+; □) after 0, 5, 9, 14, and 19 days of treatment. Fold increase in cell number was calculated relative to the initial cell number at day 0. Results are expressed as mean ± SEM. ***$p < 0.001$ vs C−, Hp7G1, and Hp7G10.

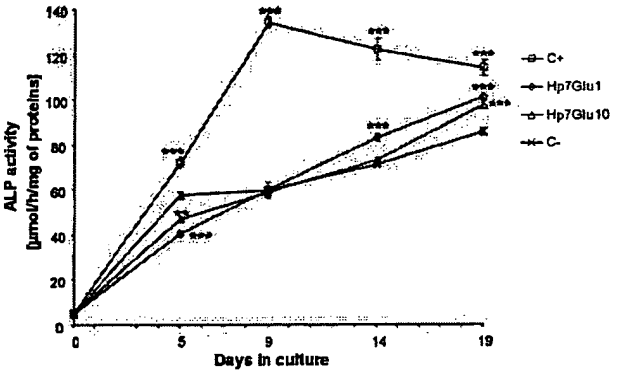

Figure 4. ALP activity of primary osteoblasts cultured in minimal medium (C−; ×), supplemented with 1 μM (Hp7G1; ◇) or 10 μM (Hp7G10; △) hesperetin 7-*O*-glucuronide, or in optimized medium (C+; □) after 0, 5, 9, 14, and 19 days of treatment. Results are expressed as mean ± SEM. **$p < 0.01$, ***$p < 0.001$ vs C−.

the absence of cells (0.34%), but the extent of hydrolysis was clearly lower than that in the presence of cells. Furthermore, traces of Hp7G were detected in the cell lysate after 24 h-exposure (Figure 2C), even though the concentration was below our quantification limit. Hp was not detected in the cell lysate. Our data thus suggest a very limited but existing penetration of Hp7G in primary rat osteoblasts or interaction of Hp7G with the membrane of osteoblasts.

Cell Proliferation. Impact of Hp7G on cell proliferation on days 0, 5, 9, 14, and 19 was assessed (Figure 3). As expected, increased proliferation was observed until day 5 and remained unchanged after this time in C+ conditions. While a significantly higher proliferation rate was observed in this condition compared to that in the others ($p < 0.001$), Hp7G did not influence proliferation.

Osteoblast Differentiation (ALP Activity). Osteoblast differentiation was assessed kinetically by measuring ALP activity in cells treated for 19 days.

In osteoblasts treated with ascorbic acid and β-glycerophosphate (C+), ALP activity (Figure 4) was significantly increased compared to that in minimal medium (C−) from day 5 up to day 19 ($p < 0.001$). Hp7G at 1 μM (Hp7G1) and 10 μM (Hp7G10) at day 5 decreased ALP activity when compared to C− ($p < 0.01$). However, when Hp7G was added at 1 μM, a significant increase of ALP activity on days 14 and 19 was observed (D14, +16.6%; D19, +18%; $p < 0.001$ vs C−), while only a significant increase was noted on day 19 with the higher dose (D19, +14%; $p < 0.001$ vs C−) (Figure 4).

Gene Expression (Real-Time PCR). The changes in gene expression were considered significant when 20% up (1.20-fold)- or down (1.20-fold)-regulation was obtained, compared to that of C− (value = 1.00).

Runx2 and Osterix Expression. While Runx2 expression was significantly decreased in C+ and Hp7G10 conditions after 24 h of exposure, an increased Runx2 messenger level was measured after 48 h, whatever the treatment (C+, 1.94-fold; Hp7G1, 2.66-fold; Hp7G10, 2.45-fold; $p < 0.05$ vs C−) (Figure 5A). Concerning Osterix, no effect from the treatments was observed after 24 h of culture. However, a decreased mRNA level was reported in C+ conditions (1.61-fold down-regulated; $p < 0.05$ vs C−), while Hp7G at both doses was able to up-regulate Osterix expression after 48 h of exposure (Hp7G1, 1.32-fold; Hp7G10, 1.40-fold; $p < 0.05$ vs C−) (Figure 5A).

OPG and RANKL Expression. Expression of OPG was significantly down-regulated in C+ medium at both times of treatment (24 h, 1.96-fold; 48 h, 1.33-fold; $p < 0.05$ vs C−). The OPG transcript level remained unchanged after Hp7G treatment. Concerning RANKL, after 24 h of treatment, the mRNA level remained unchanged in C+ conditions and was decreased only by Hp7G10 (1.25-fold; $p < 0.05$ vs C−). However, after 48 h of treatment, the decrease was observed in every condition at the same rate, even in C+ medium (2.00-fold; $p < 0.05$ vs C−) (Figure 5B).

Noggin, BMP2, and BMP4 expression. The expression of Noggin was strongly down-regulated in C+ medium whatever the time of exposure (24 h, 3.56-fold; 48 h, 15.60-fold; $p < 0.05$ vs C−). Hp7G, at both doses, was also able to significantly decrease Noggin mRNA level after 24 h (Hp7G1, 1.23-fold; Hp7G10, 1.27-fold; $p < 0.05$ vs C−) and 48 h of treatment (Hp7G1, 1.61-fold; Hp7G10, 1.70-fold; $p < 0.05$ vs C−) (Table 2).

Regarding BMP2 and BMP4, only BMP4 mRNA level after 24 h of treatment was significantly up-regulated in C+ medium (1.47-fold; $p < 0.05$ vs C−). After 24 h of exposure, BMP2 and BMP4 expression was not affected by Hp7G treatment, while after 48 h, a decreased BMP2 messenger level was measured for Hp7G1 (1.45-fold down-regulated; $p < 0.05$ vs C−) (Table 2).

Smad1 and Smad5 Expression. Expression of both genes was down-regulated in C+ medium ($p < 0.05$ vs C−). Smad1 transcript level was not changed by Hp7G treatment, while Hp7G at both doses down-regulated Smad5 expression after 24 h (1.23-fold; $p < 0.05$ vs C−); an increase was observed after 48 h of exposure (Table 2).

c-Jun and c-fos Expression. No significant difference in c-Jun expression was observed, whatever treatment and time of exposure. Regarding c-fos expression, only Hp7G1 was able to decrease the mRNA level after 24 h of treatment (1.23-fold; $p < 0.05$ vs C−) (Table 2).

ALP, OPN, and OCN Expression. ALP expression was not affected after 24 h of treatment. However, after 48 h of exposure, expression of ALP was upregulated in all conditions (C+, 1.30-fold; Hp7G1, 1.45-fold; Hp7G10, 1.39-fold; $p < 0.05$ vs C−) (Table 2).

In the C+ medium, while a significant decrease of OPN expression was observed at both times, OCN expression was strongly upregulated (24 h, 2.20-fold; 48 h, 9.45-fold; $p < 0.05$ vs C−). Hp7G did not have any influence on OPN expression whatever the dose and time of exposure. OCN expression was significantly upregulated in Hp7G10 (1.31-fold; $p < 0.05$ vs C−) after 48 h of treatment (Table 2).

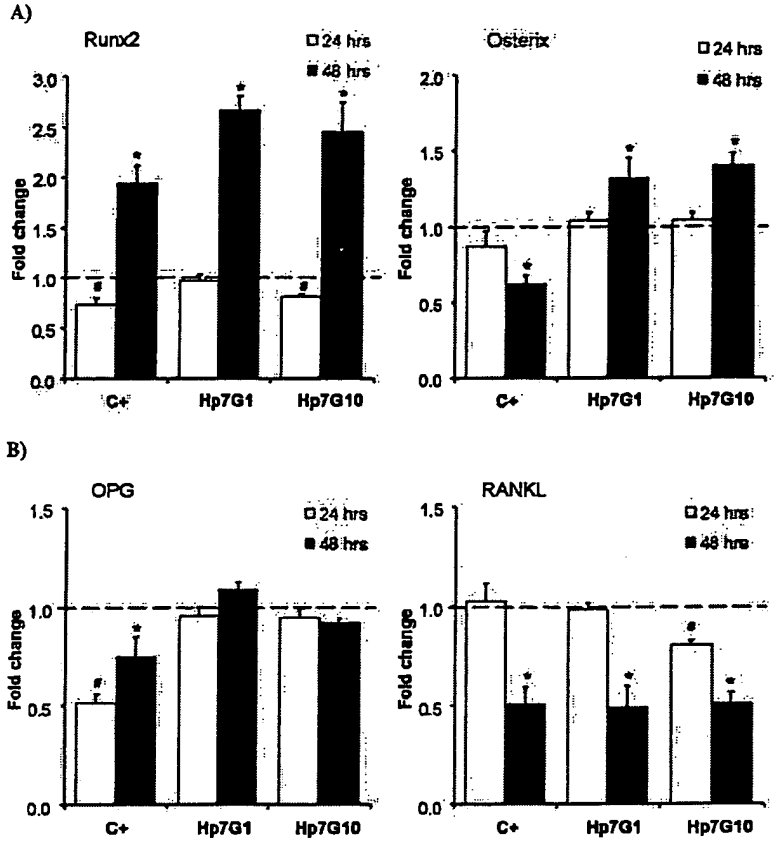

Figure 5. Gene expression of (A) Runx2 and Osterix (B) OPG and RANKL in primary osteoblasts cultured in minimal medium (C−), supplemented with 1 μM (Hp7G1) or 10 μM (Hp7G10) hesperetin 7-*O*-glucuronide, or in optimized medium (C+). Results are presented as fold change compared to C− (dashed line) after 24 and 48 h of exposure. Results are expressed as mean ± SEM. $^{\#}p < 0.05$ vs C− 24 h; $^{*}p < 0.05$ vs C− 48 h.

Table 2. Expression of Osteoblast-Related Genes[a]

gene	time of exposure	fold change C+	Hp7G1	Hp7G10
Noggin	24 h	0.28 ± 0.02#	0.81 ± 0.06#	0.78 ± 0.05#
	48 h	0.06 ± 0.01*	0.62 ± 0.05*	0.59 ± 0.11*
BMP2	24 h	1.23 ± 0.22	0.97 ± 0.08	0.92 ± 0.04
	48 h	1.24 ± 0.10	0.69 ± 0.08*	0.97 ± 0.03
BMP4	24 h	1.47 ± 0.07#	0.96 ± 0.06	0.99 ± 0.08
	48 h	1.00 ± 0.05	1.14 ± 0.14	0.86 ± 0.05
Smad1	24 h	0.76 ± 0.06#	0.95 ± 0.02	1.00 ± 0.02
	48 h	0.69 ± 0.02*	0.91 ± 0.02	0.83 ± 0.06
Smad5	24 h	0.72 ± 0.09#	0.81 ± 0.03#	0.81 ± 0.02#
	48 h	0.94 ± 0.03	1.45 ± 0.13*	1.17 ± 0.06
c-Jun	24 h	1.22 ± 0.17	0.95 ± 0.03	0.98 ± 0.04
	48 h	0.84 ± 0.17	0.96 ± 0.05	1.00 ± 0.14
c-fos	24 h	1.17 ± 0.21	0.81 ± 0.01#	0.86 ± 0.05
	48 h	0.91 ± 0.07	0.97 ± 0.03	0.91 ± 0.02
ALP	24 h	0.93 ± 0.06	0.85 ± 0.02	0.89 ± 0.05
	48 h	1.27 ± 0.08*	1.56 ± 0.09*	1.39 ± 1.39*
OPN	24 h	0.76 ± 0.09#	0.91 ± 0.05	0.96 ± 0.02
	48 h	0.68 ± 0.02*	1.00 ± 0.05	0.95 ± 0.08
OCN	24 h	2.20 ± 0.15#	1.00 ± 0.17	0.91 ± 0.06
	48 h	9.45 ± 0.40*	1.40 ± 0.42	1.31 ± 0.10*

[a] Primary osteoblasts cultured in minimal medium (C−), supplemented with 1 μM (Hp7G1) or 10 μM (Hp7G10) hesperetin 7-*O*-glucuronide or in optimized medium (C+) after 24 h and 48 h of exposure. Results are presented as fold change compared to C− (value = 1.00) after 24 or 48 h of exposure. Results are expressed as mean ± SEM. $^{\#}p < 0.05$ vs C− 24 h. $^{*}p < 0.05$ vs C− 48 h.

Effect of Hp7G on the Phosphorylation of Smad1/5/8 and ERK1/2 Proteins. Phosphorylation of Smad1/5/8 and ERK1/2 proteins was assessed by Western blotting on cell lysates from cells treated for 24 and 48 h (Figure 6A and B). The antibodies anti-Smad1/5/8 and antiphospho-Smad1/5/8 used in the Western blot analysis can recognize three Smad proteins, 1, 5, and 8. Because of the specificity of antibodies as well as the expression of proteins, two or three bands may be visible.

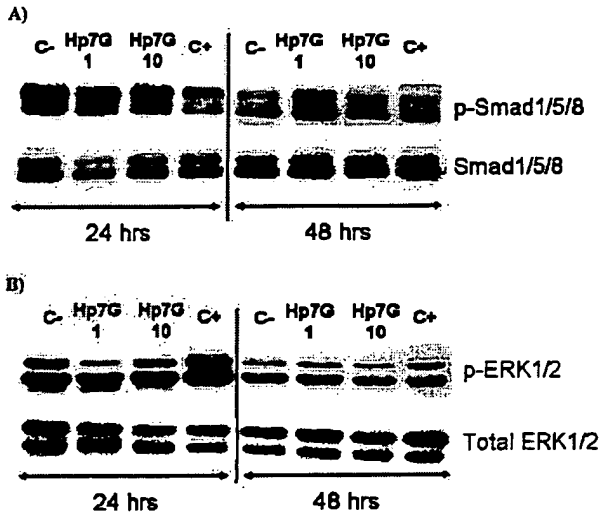

Figure 6. Phosphorylation of (A) Smad1/5/8 proteins and (B) ERK1/2 proteins in primary osteoblasts cultured in minimal medium (C−), supplemented with 1 μM (Hp7G1) or 10 μM (Hp7G10) hesperetin 7-*O*-glucuronide, or in optimized medium (C+) after 24 and 48 h of exposure.

The observations reported here are qualitative and not quantitative.

C+ and Hp7G at both doses could decrease the phosphorylation of Smad1/5/8 after 24 h of treatment; the strongest effect was obtained with Hp7G1. On the contrary, after 48 h of exposure, phosphorylation of Smad1/5/8 seemed to be enhanced by Hp7G1 (Figure 6A).

Concerning ERK1/2, phosphorylation was decreased in Hp7G conditions compared to that in C−, while no difference between C− and C+ was detected after 24 h of exposure. Phosphorylation of ERK1/2 after 48 h of treatment was lower than that after 24 h of exposure, and moreover, no differences between conditions could be detected (Figure 6B).

DISCUSSION

It has been previously demonstrated that hesperetin (aglycone form of hesperidin) can influence bone formation via stimulation of osteoblast differentiation mainly through the BMP pathway (*7*). In this study, we focused on the potential effects of hesperetin-7-*O*-glucuronide, its main metabolite, on the same experimental model. Indeed, the circulating forms may possess different biological properties within cells and tissues compared to those of polyphenol aglycones (*24*).

Cellular Uptake. Activation of cell signaling can occur via different ways including an interaction of a compound with a receptor on the cell surface and/or by interaction with extracellular proteins (*9*). However, some nutrients which are able to enter cells through a transporter mediated process or by passive diffusion may directly interact with transcription factors, thus affecting the target gene expression (*25*). It has been shown that aglycone forms of flavonoids can cross cell membranes by passive diffusion, whereas conjugates need active transport (*9*, *26*). In primary rat osteoblasts, we observed that the cellular uptake of Hp was definitely more efficient than that of Hp7G, which was too limited to be unambiguously demonstrated in our conditions. We only observed (i) a small increase of Hp7G hydrolysis in the medium when cells were present compared to when Hp7G was incubated in cell-free medium and (ii) traces of Hp7G in the cell extract after 24 h of exposure to glucuronide, which may also reflect binding to cell membranes. Primary cell osteoblasts may lack efficient transporters to facilitate the uptake of flavonoid glucuronides. However, these cells were shown to export Hp7G in the medium after Hp exposure (**Figure 1**), which shows that primary osteoblasts are able to glucuronide Hp as shown for Caco-2 cells (*27*, *28*) and fibroblasts (*11*), and possess transporters to efficiently export flavonoid glucuronides. Our results thus suggest a very transient presence of Hp7G inside the primary rat osteoblasts after either Hp or Hp7G exposure. This transient presence was nevertheless associated with a positive effect on cell differentiation when osteoblasts were exposed to glucuronide.

Effect of Hp7G on Osteoblast Proliferation and Differentiation. This study has assessed the impact of a hesperetin conjugate on osteoblast cells at nutritional and physiological concentrations (1 and 10 μM). The choice of nutritional doses led to significant cellular responses but were quite small.

In our experimental conditions, Hp7G, similarly to its aglycone form (*7*, *29*) and to other polyphenols (*30*−*32*), did not affect osteoblast proliferation (**Figure 3**) but was able to influence osteoblast differentiation (**Figure 4**). Even if Hp7G decreased ALP activity on day 5, which could reflect a faster commitment of these cells compared to the cells cultivated in minimal medium (*33*), the final effect of treatment is crucial to interpret results. Hp7G at 1 μM (on days 14 and 19) and 10 μM (on day 19) increased ALP activity, which can also play a role in osteoblast mineralization probably by a release of the phosphate necessary for calcium nodule formation (*34*, *35*). Surprisingly, Hp7G1 was more efficient than Hp7G10, whereas hesperetin at the 10 μM dose was more efficient than 1 μM (*7*). Moreover, Hp7G1 increased ALP activity from day 14, while Hp7G10 was only at day 19. Again, this was inversed when cells were exposed to hesperetin (*7*). In other studies, similar dose-dependent patterns of ALP activity in osteoblasts exposed to different aglycone compounds were reported (*30*, *36*); however, data with their corresponding metabolites are still lacking. This is probably because conjugated molecules are not commercialized (*24*). However, the glucuronide form of hesperetin was more efficient than the aglycone parent form in stimulating osteoblast differentiation as previously assessed (*7*). The same observation was reported for quercetin and its glucuronide in HUVEC cells (*37*). This kind of experiment supports the fact that conjugates can share physiological bioactivities, even if they are poorly or not absorbed by cells (*28*).

Possible Signaling Pathways Involved in Hp7G Action. Gene expression was analyzed after 24 and 48 h of exposure. In our experimental conditions, a stronger effect on gene expression was observed after 48 h of treatment (**Figure 5** and **Table 2**), suggesting that the duration of exposure may influence the gene response. For almost all genes evaluated, the level of mRNA appeared to be similar for 1 and 10 μM Hp7G. It can be hypothesized that the effective dose of Hp7G to modulate bone related genes in primary osteoblasts is 1 μM, this being consistent with ALP findings (**Figure 3**). However, this does not exclude the higher efficacy of a lower dose of glucuronide and should therefore be evaluated.

In our experimental conditions, ALP and OCN mRNA levels were increased after 48 h of Hp7G treatment (**Table 2**). Expression of these genes may be regulated by Runx2 (*38*). Moreover, Hp7G was able to upregulate the expression of not only Runx2 but also Osterix (**Figure 5A**), which are two main transcription factors related to osteoblasts (*14*) and are involved in BMP (*39*) and MAPK signaling (*15*, *40*). Similar results were obtained for some polyphenol aglycones such as hesperetin (*7*), resveratrol (*41*), and epigallocatechin gallate (EGCG) (*42*).

Mechanisms of interaction with Runx2 are complex, including binding of components such as AP-1 factors and Smad proteins to DNA regions in target gene promoters. Regarding Smad phosphorylation, Hp7G1 seemed to increase the phosphorylation of the Smad1/5/8 complex after 48 h of exposure (**Figure 6A**). This result is consistent with those of several authors who have demonstrated the possible phosphorylation of the Smad1/5/8 complex in osteoblasts treated with some polyphenols such as myricetin (*30*) and coumarin derivates (*31*, *43*). This suggests that the BMP pathway via the activation of Smad1/5/8 may be implicated in Hp7G action even if BMP2 and BMP4 gene expression was not increased (**Table 2**), contrary to previous findings concerning some polyphenols (*30*, *31*, *36*, *43*, *44*) including hesperetin (*7*). This could be due to the fact that aglycones and not conjugates were used. However, in this study, the hesperetin metabolite decreased expression of Noggin, one of the osteoblast secreted proteins which can limit the level of BMP signals (*45*), supporting the hypothesized interaction of hesperetin glucuronide with the BMP pathway.

The effects of Hp7G on c-Jun and c-fos (components of complex AP-1), and on ERK1/2, both implicated in the MAPK cascade, were assessed. In our experimental design, the glucuronide could only slightly decrease c-fos gene expression and was able to decrease the phosphorylation of ERK1/2 after 24 h of exposure, while no effect after 48 h was reported (**Figure 6B**). On the contrary, it has been shown that some coumarin aglycones at 10 μM were able to stimulate the phosphorylation of ERK1/2 in primary rat osteoblasts after 12 h of exposure (*31*). However, the

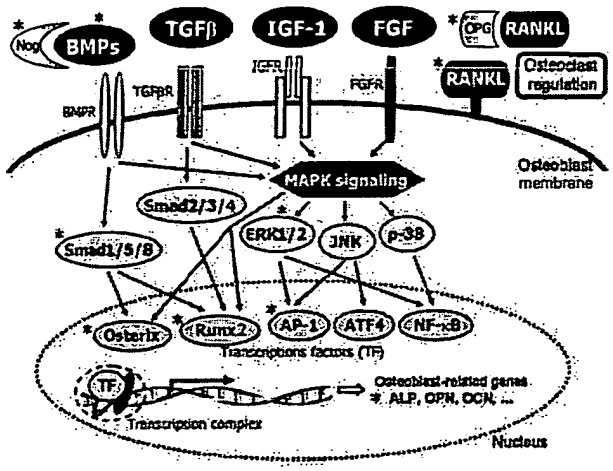

Figure 7. Signaling pathways implicated in the regulation of osteoblast differentiation. Asterisks (*) mark the obtained effect of hesperetin-7-*O*-glucuronide (Hp7G) on gene expression involved in osteoblast differentiation, in our experimental conditions (see Table 2 and Figure 5 for details).

phosphorylation of ERK1/2 in MC3T3-E1 osteoblast exposure to EGCG (10−30 μM) for 60 min remained unchanged compared to that of nontreated cells (*46*). Regarding our results, it is difficult to draw a clear conclusion about an interaction of Hp7G with MAPK signaling. It could be possible that aglycone forms can activate MAPK signaling including JNK, ERK1/2, and p-38 MAPK because they activate some of the phase II drug-metabolizing enzymes which are responsible for their conjugation (*47*). In the case of glucuronides, these enzymes are not necessary. This could explain why Hp7G failed to activate MAPK/ERK signaling. Thus, different signaling pathways may be activated compared to those in aglycones.

A further important outcome of this study is the finding that the hesperetin conjugate is able to decrease the gene expression of RANKL while at the same time not change OPG expression (Figure 5B). These results suggest that Hp7G may be able to limit osteoclast activation, as previously shown for daidzein and genistein (*48*).

Conclusions. Our data demonstrated that hesperetin glucuronide is able to affect osteoblast differentiation at nutritional and physiological doses. Indeed, Hp7G may act on osteoblasts mainly through Runx2 and Osterix activation by molecular mechanisms not well identified (Figure 7). It is possible that these transcription factors could interact with the BMP cascade and/or MAPK signaling. However, further mechanistic studies are necessary to confirm this hypothesis.

ABBREVIATIONS USED

ALP, alkaline phosphatase; AP-1, activator protein 1; BMP, bone morphogenetic protein; ERK, extracellular signal-regulated kinase; Hp, hesperetin; Hp7G, hesperetin-7-*O*-glucuronide; JNK, c-Jun N-terminal kinase; MAPK, mitogen-activated protein kinase; OCN, osteocalcin; OPG, osteoprotegerin; OPN, osteopontin; RANKL, receptor activator of nuclear factor-kappaB (RANK) ligand.

LITERATURE CITED

(1) Manach, C.; Morand, C.; Gil-Izquierdo, A.; Bouteloup-Demange, C.; Remesy, C. Bioavailability in humans of the flavanones hesperidin and narirutin after the ingestion of two doses of orange juice. *Eur. J. Clin. Nutr.* **2003**, *57*, 235–242.

(2) Matsumoto, H.; Ikoma, Y.; Sugiura, M.; Yano, M.; Hasegawa, Y. Identification and quantification of the conjugated metabolites derived from orally administered hesperidin in rat plasma. *J. Agric. Food Chem.* **2004**, *52*, 6653–9.

(3) Chiba, H.; Uehara, M.; Wu, J.; Wang, X. X.; Masuyama, R.; Suzuki, K.; Kanazawa, K.; Ishimi, Y. Hesperidin, a citrus flavonoid, inhibits bone loss and decreases serum and hepatic lipids in ovariectomized mice. *J. Nutr.* **2003**, *133*, 1892–1897.

(4) Horcajada, M. N.; Habauzit, V.; Trzeciakiewicz, A.; Morand, C.; Gil-Izquierdo, A.; Mardon, J.; Lebecque, P.; Davicco, M. J.; Chee, W. S.; Coxam, V.; Offord, E. Hesperidin inhibits ovariectomized-induced osteopenia and shows differential effects on bone mass and strength in young and adult intact rats. *J. Appl. Physiol.* **2008**, *104*, 648–654.

(5) Garg, A.; Garg, S.; Zaneveld, L. J. D.; Singla, A. K. Chemistry and pharmacology of the citrus bioflavonoid hesperidin. *Phytother Res.* **2001**, *15*, 655–669.

(6) Deyhim, F.; Garica, K.; Lopez, E.; Gonzalez, J.; Ino, S.; Garcia, M.; Patil, B. S. Citrus juice modulates bone strength in male senescent rat model of osteoporosis. *Nutrition* **2006**, *22*, 559–563.

(7) Trzeciakiewicz, A.; Habauzit, V.; Mercier, S.; Lebecque, P.; Davicco, M. J.; Demigne, C.; Horcajada, M. N. Hesperetin stimulates differentiation of primary rat osteoblasts involving the BMP signalling pathway. *J. Nutr. Biochem.* [Online early access]. DOI: 10.1016/j.nutbio.2009.01.017.

(8) Xu, C.; Li, C. Y.; Kong, A. N. Induction of phase I, II and III drug metabolism/transport by xenobiotics. *Arch. Pharm. Res.* **2005**, *28*, 249–68.

(9) Williamson, G.; Barron, D.; Shimoi, K.; Terao, J. In vitro biological properties of flavonoid conjugates found in vivo. *Free Radical Res.* **2005**, *39*, 457–469.

(10) Kim, D. S.; Takai, H.; Arai, M.; Araki, S.; Mezawa, M.; Kawai, Y.; Murota, K.; Terao, J.; Ogata, Y. Effects of quercetin and quercetin 3-glucuronide on the expression of bone sialoprotein gene. *J. Cell Biochem.* **2007**, *101*, 790–800.

(11) Proteggente, A. R.; Basu-Modak, S.; Kuhnle, G.; Gordon, M. J.; Youdim, K.; Tyrrell, R.; Rice-Evans, C. A. Hesperetin glucuronide, a photoprotective agent arising from flavonoid metabolism in human skin fibroblasts. *Photochem. Photobiol.* **2003**, *78*, 256–261.

(12) Vauzour, D.; Vafeiadou, K.; Rice-Evans, C.; Williams, R. J.; Spencer, J. P. E. Activation of pro-survival Akt and ERK1/2 signalling pathways underlie the anti-apoptotic effects of flavanones in cortical neurons. *J. Neurochem.* **2007**, *103*, 1355–1367.

(13) Trzeciakiewicz, A.; Habauzit, V.; Horcajada, M. N. When nutrition interacts with osteoblast function: molecular mechanisms of polyphenols. *Nutr. Res. Rev.* **2009**, 1–15.

(14) Marie, P. J. Transcription factors controlling osteoblastogenesis. *Arch. Biochem. Biophys.* **2008**, *473*, 98–105.

(15) Franceschi, R. T.; Xiao, G. Z. Regulation of the osteoblast-specific transcription factor, runx2: Responsiveness to multiple signal transduction pathways. *J. Cell Biochem.* **2003**, *88*, 446–454.

(16) Miyazono, K.; Maeda, S.; Imamura, T. BMP receptor signaling: Transcriptional targets, regulation of signals, and signaling cross-talk. *Cytokine Growth Factor Rev.* **2005**, *16*, 251–63.

(17) De Wilde, A.; Lieberherr, M.; Colin, C.; Pointillart, A. A low dose of daidzein acts as an ERbeta-selective agonist in trabecular osteoblasts of young female piglets. *J. Cell Physiol.* **2004**, *200*, 253–262.

(18) Pang, J. L.; Ricupero, D. A.; Huang, S.; Fatma, N.; Singh, D. P.; Romero, J. R.; Chattopadhyay, N. Differential activity of kaempferol and quercetin in attenuating tumor necrosis factor receptor family signaling in bone cells. *Biochem. Pharmacol.* **2006**, *71*, 818–26.

(19) Boyce, B. F.; Xing, L. P. Functions of RANKL/RANK/OPG in bone modeling and remodeling. *Arch. Biochem. Biophys.* **2008**, *473*, 139–146.

(20) Boumendjel, A.; Blanc, M.; Williamson, G.; Barron, D. Efficient synthesis of flavanone glucuronides. *J. Agric. Food Chem.* **2009**, *57*, 7264–7267.

(21) Declercq, H.; Van den Vreken, N.; De Maeyer, E.; Verbeeck, R.; Schacht, E.; De Ridder, L.; Cornelissen, M. Isolation, proliferation and differentiation of osteoblastic cells to study cell/biomaterial interactions: comparison of different isolation techniques and source. *Biomaterials* **2004**, *25*, 757–768.

(22) Sabokbar, A.; Millett, P. J.; Myer, B.; Rushton, N. A rapid, quantitative assay for measuring alkaline-phosphatase activity in osteoblastic cells in-vitro. *Bone Miner.* 1994, *27*, 57–67.

(23) Livak, K. J.; Schmittgen, T. D. Analysis of relative gene expression data using real-time quantitative PCR and the 2(-delta delta C(T)) method. *Methods* 2001, *25*, 402–8.

(24) Kroon, P. A.; Clifford, M. N.; Crozier, A.; Day, A. J.; Donovan, J. L.; Manach, C.; Williamson, G. How should we assess the effects of exposure to dietary polyphenols in vitro? *Am. J. Clin. Nutr.* 2004, *80*, 15–21.

(25) Muller, M.; Kersten, S. Nutrigenomics: goals and strategies. *Nat. Rev. Genet.* 2003, *4*, 315–22.

(26) Morris, M. E.; Zhang, S. Flavonoid-drug interactions: effects of flavonoids on ABC transporters. *Life Sci.* 2006, *78*, 2116–30.

(27) Brand, W.; van der Wel, P. A. I.; Rein, M. J.; Barron, D.; Williamson, G.; van Bladeren, P. J.; Rietjens, I. Metabolism and transport of the citrus flavonoid hesperetin in Caco-2 cell monolayers. *Drug Metab. Dispos.* 2008, *36*, 1794–1802.

(28) Serra, H.; Mendes, T.; Bronze, M. R.; Simplicio, A. L. Prediction of intestinal absorption and metabolism of pharmacologically active flavones and flavanones. *Bioorg. Med. Chem.* 2008, *16*, 4009–4018.

(29) Choi, E. M.; Kim, Y. H. Hesperetin attenuates the highly reducing sugar-triggered inhibition of osteoblast differentiation. *Cell Biol. Toxicol.* 2008, *24*, 225–31.

(30) Hsu, Y. L.; Chang, J. K.; Tsai, C. H.; Chien, T. T. C.; Kuo, P. L. Myricetin induces human osteoblast differentiation through bone morphogenetic protein-2/p38 mitogen-activated protein kinase pathway. *Biochem. Pharmacol.* 2007. *73*, 504–514.

(31) Tang, C. H.; Yang, R. S.; Chien, M. Y.; Chen, C. C.; Fu, W. M. Enhancement of bone morphogenetic protein-2 expression and bone formation by coumarin derivatives via p38 and ERK-dependent pathway in osteoblasts. *Eur. J. Pharmacol.* 2008, *579*, 40–49.

(32) Zhao, J.; Ohba, S.; Shinkai, M.; Chung, U. I.; Nagamune, T. Icariin induces osteogenic differentiation in vitro in a BMP- and Runx2-dependent manner. *Biochem. Biophys. Res. Commun.* 2008, *369*, 444–448.

(33) Aubin, J. E. Advances in the osteoblast lineage. *Biochem. Cell Biol.* 1998, *76*, 899–910.

(34) Siffert, R. S. The role of alkaline phosphatase in osteogenesis. *J. Exp. Med.* 1951, *93*, 415–426.

(35) Sugawara, Y.; Suzuki, K.; Koshikawa, M.; Ando, M.; Iida, J. Necessity of enzymatic activity of alkaline phosphatase for mineralization of osteoblastic cells. *Jpn. J. Pharmacol.* 2002, *88*, 262–269.

(36) Chang, J. K.; Hsu, Y. L.; Teng, I. C.; Kuo, P. L. Piceatannol stimulates osteoblast differentiation that may be mediated by increased bone morphogenetic protein-2 production. *Eur. J. Pharmacol.* 2006, *551* (1–3), 1–9.

(37) Tribolo, S.; Lodib, F.; Connor, C.; Suri, S.; Wilson, V. G.; Taylor, M. A.; Needs, P. W.; Kroon, P. A.; Hughes, D. A. Comparative effects of quercetin and its predominant human metabolites on adhesion molecule expression in activated human vascular endothelial cells. *Atherosclerosis* 2008, *197*, 50–56.

(38) Ducy, P.; Zhang, R.; Geoffroy, V.; Ridall, A. L.; Karsenty, G. Osf2/Cbfa1: a transcriptional activator of osteoblast differentiation. *Cell* 1997, *89*, 747–54.

(39) Yamaguchi, A.; Komori, T.; Suda, T. Regulation of osteoblast differentiation mediated by bone morphogenetic proteins, hedgehogs, and Cbfa1. *Endocr. Rev.* 2000, *21*, 393–411.

(40) Celil, A. B.; Hollinger, J. O.; Campbell, P. G. Osx transcriptional regulation is mediated by additional pathways to BMP2/Smad signaling. *J. Cell Biochem.* 2005, *95*, 518–528.

(41) Dai, Z.; Li, Y.; Quarles, L. D.; Song, T.; Pan, W.; Zhou, H.; Xiao, Z. Resveratrol enhances proliferation and osteoblastic differentiation in human mesenchymal stem cells via ER-dependent ERK1/2 activation. *Phytomedicine* 2007, *14*, 806–814.

(42) Chen, C. H.; Ho, M. L.; Chang, J. K.; Hung, S. H.; Wang, G. J. Green tea catechin enhances osteogenesis in a bone marrow mesenchymal stem cell line. *Osteoporosis Int.* 2005, *16*, 2039–2045.

(43) Kuo, P.-L.; Hsu, Y.-L.; Chang, C.-H.; Chang, J.-K. Ostholemediated cell differentiation through bone morphogenetic protein-2/p38 and extracellular signal-regulated kinase 1/2 pathway in human osteoblast cells. *J. Pharmacol. Exp. Ther.* 2005, *314*, 1290–1299.

(44) Zhao, J.; Ohba, S.; Shinkai, M.; Chung, U. I.; Nagamune, T. Icariin induces osteogenic differentiation in vitro in a BMP- and Runx2-dependent manner. *Biochem. Biophys. Res. Commun.* 2008, *369*, 444–8.

(45) Groppe, J.; Greenwald, J.; Wiater, E.; Rodriguez-Leon, J.; Economides, A. N.; Kwiatkowski, W.; Affolter, M.; Vale, W. W.; Belmonte, J. C. I.; Choe, S. Structural basis of BMP signalling inhibition by the cystine knot protein Noggin. *Nature* 2002, *420*, 636–642.

(46) Hayashi, K.; Takai, S.; Matsushima-Nishiwaki, R.; Hanai, Y.; Kato, K.; Tokuda, H.; Kozawa, O. (−)-Epigallocatechin gallate reduces transforming growth factor beta-stimulated HSP27 induction through the suppression of stress-activated protein kinase/c-Jun N-terminal kinase in osteoblasts. *Life Sci.* 2008, *82*, 1012–1017.

(47) Kong, A. N.; Owuor, E.; Yu, R.; Hebbar, V.; Chen, C.; Hu, R.; Mandlekar, S. Induction of xenobiotic enzymes by the MAP kinase pathway and the antioxidant or electrophile response element (ARE/EpRE). *Drug Metab. Rev.* 2001, *33*, 255–71.

(48) Chen, X. W.; Garner, S. C.; Anderson, J. J. Isoflavones regulate interleukin-6 and osteoprotegerin synthesis during osteoblast cell differentiation via an estrogen-receptor-dependent pathway. *Biochem. Biophys. Res. Commun.* 2002, *295*, 417–22.

Received for review July 31, 2009. Revised manuscript received November 7, 2009. Accepted November 09, 2009.